CALIBRATION OF HOT-FILM X-PROBES FOR HIGH ACCURACY ANGLE

ALIGNMENT IN WIND TUNNELS

by

Dallin L. Jackson

A thesis submitted in partial fulfillment
of the requirements for the degree

of

MASTER OF SCIENCE

in

Mechanical Engineering

Approved:

_____   _____
Thomas Fronk, Ph.D.   David Geller, Ph.D.
Major Professor   Committee Member

_____   _____
Steven Folkman, Ph.D.   Richard S. Inouye, Ph.D.
Committee Member   Vice Provost for Graduate Studies

UTAH STATE UNIVERSITY
Logan, Utah

2019

ABSTRACT

Calibration of Hot-Film X-Probes for High Accuracy Angle Alignment in Wind Tunnels

by

Dallin L. Jackson, Master of Science

Utah State University, 2019

Major Professor: Thomas Fronk, Ph.D.
Department: Mechanical and Aerospace Engineering

The alignment of a mounting plate as well as the calibration of the test section velocity on a wind tunnel at Hill Air Force Base is performed using a hot-film anemometer probe. Since the wind tunnel is used for calibration of F-16 Angle of Attack Transmitters, the requirements for this alignment are very tight. Jorgensen's equation and a look-up table are investigated as calibration candidates to meet these requirements. The importance of calibration and measurement conditions are shown to be of more importance than the calibration method to obtain consistent results between multiple probes. Results show that although measurements could be validated after calibration, hot-film probe measurements are not consistent with each other. Possible solutions to reduce these inconsistencies are discussed, as well as alternate calibration methods to achieve the wind tunnel requirements.

(112 pages)

PUBLIC ABSTRACT

Calibration of Hot-Film X-Probes for High Accuracy Angle Alignment in Wind Tunnels

Dallin L. Jackson

This thesis investigates the use of hot-film thermal anemometers to align a plate on a wind tunnel at Hill Air Force Base that is used to calibrate Angle of Attack Transmitters on F-16s. A reoccuring problem with this wind tunnel is that no two instruments can verify an angle reading of the the mounting plate for the Angle of Attack Transmitters to the air stream in the wind tunnel. Multiple thermal anemometer calibration methods, such as Jorgensen's equation and a look-up table are implemented to attemp to achieve consistent measurements between multiple probes. The results show that it is neccessary to have conditions match between calibration and measurement when attempting to achieve high accuracy with angle measurements.

To my wife Jessie and son Liam. Anything is possible with hard work, sweat, and tears....

ACKNOWLEDGMENTS

Thank you to all of the people who helped me on this project. Specifically, thank you to Seth Sherman for all of your hard work over the years on this project and listening to my crazy ideas. To Maddie Dziuk for your help on writing code to get the results I needed. To my mom, Shelley Jackson for your many hours of proofreading and grammar checking. Lastly, to my wife Jessie, for your love and patience, and giving me the motivation and encouragement I always need.

Dallin L. Jackson

CONTENTS

LIST OF TABLES

LIST OF FIGURES

ACRONYMS

AFB   air force base

ANSI   American National Standards Institute

AOAT   angle of attack transmitter

BNC   Bayonet Neill–Concelman (connecter)

CCA   constant current anemometer

CTA   constant temperature anemometer

DAQ   data acquisition

DMM   digital multi-meter

LDA   laser doppler anemometer

NCSL   National Conference of Standards Laboratories

TO   technical order

TUR   test uncertainty ratio

UUT   unit under test

VFD   variable frequency device

CHAPTER 1

Introduction

1.1   Introduction

The maintenance depot at Hill Air Force Base (AFB), Utah performs various repairs and calibrations on multiple aircraft instruments. One such instrument is the Angle of Attack Transmitter (AOAT) used on the General Dynamics Fighting Falcon, commonly known as the F-16. The AOAT is an important safety instrument, as it helps prevent stall by displaying to the pilot the angle of attack, or the angle between the flight direction and nose of the aircraft. The F-16 AOAT must pass a static friction test, which is performed by placing the AOAT in a wind tunnel with a velocity of 120 ± 5 knots and return to within $\pm 0.25°$ of the free air stream after it has been disturbed clockwise as well as counterclockwise by at least $30°$.

A wind tunnel is commonly used as a simulation device to obtain drag and lift forces by the flow of air over an aerodynamic model. The application at Hill AFB employs a wind tunnel to calibrate the AOAT on the F-16. Since this is an uncommon use for wind tunnels, it is a unique and difficult task to meet the specifications needed to certify the wind tunnel as a calibration standard.

The American National Standards Institute (ANSI) and National Conference of Standards Laboratories (NCSL) standard, ANSI/NCSL Z540.3, is used frequently by the Air Force when performing calibrations. It states that all equipment that is calibrated must allow no more than 2% false acceptance. An alternative acceptance method, according to ANSI/NCSL Z540.3, is that the calibration equipment may be four times more accurate than the tolerance requirement of an instrument. In other words, the AOAT mounting plate on the wind tunnel must be aligned to within 25% of the requirement for the F-16 AOAT to return to within $\pm 0.25°$ of the free air stream, which means that the mounting plate must

be aligned to within $\pm 0.0625°$ of the free air stream velocity in the test section of the wind tunnel.

Cost as well as accuracy were considered when designing a system capable of achieving this requirement for the alignment of the mounting plate. The design chosen that would theoretically measure accurately to within $\pm 0.0625°$ is a hot-film X-probe anemometer. This system consists of two sensors made of thin filaments which are each part of a Wheatstone bridge. A Wheatstone bridge is a circuit consisting of four resistors that are balanced with each other so that the unknown resistance of one of the four resistors can be determined. These sensors are heated to around $250°$ Celsius and when air blows across them, they are slightly cooled, which changes their resistance.

Fig. 1.1: TSI 1240-20 Hot-film probe
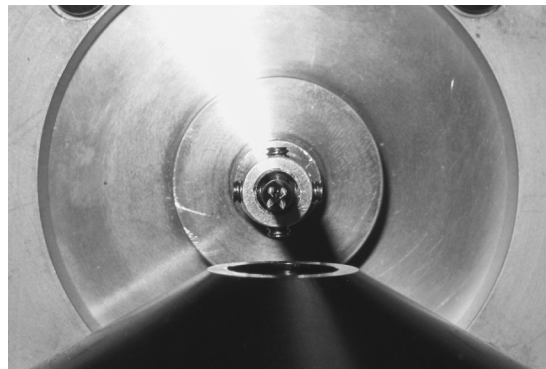
Fig. 1.2: End view of the X-probe on the modified probe support fixture on the calibrator.

A feedback amplifier is added to the Wheatstone bridge to force the resistance of the sensor to remain constant even as it is cooled. As a result, the voltage output from the Wheatstone bridge changes slightly. This produces a different voltage reading for each velocity of air applied to the X-probe and allows each velocity and voltage to be related to each other, creating a calibration method for the X-probe. Also, as the X-probe is rotated, the cooling for each sensor changes, with maximum cooling occurring when it is perpendicular to the air stream. This allows a calibration to be performed for each angle so that the probe can also read the direction of the airflow with respect to the probe.
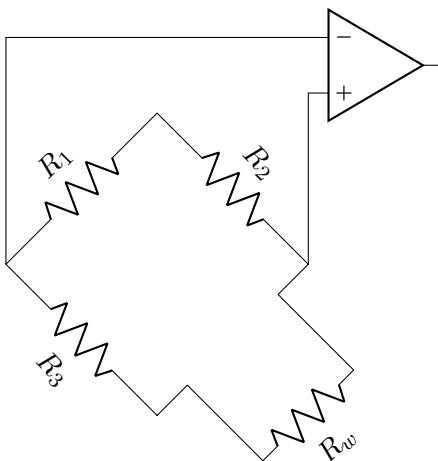
Fig. 1.3: Constant temperature anemometer wheatstone bridge circuit

Using a calibration method based on Jorgensen's equation [1], the adapter plate on the wind tunnel can be successfully aligned to $\pm 0.0625°$ of the free air stream with one probe. If the same hot-film probe is again calibrated and placed into the wind tunnel, readings would validate the previous calibration by again measuring $0° \pm 0.0625°$. However, if a second hot-film probe is calibrated and placed into the wind tunnel after the first probe was used to align the plate, the reading of the first probe could not be verified. In fact, the second probe could measure up to $0° \pm 4°$. The second probe would still be consistent with the measurements taken previously at the wind tunnel by verifying its own measurements within $\pm 0.0625°$ of the previous reading, but different hot-film probes could not be calibrated and

verify the same measurement. This inconsistency of measurements between various probes caused high uncertainty of the actual angle measurement within the wind tunnel.

In order to certify the alignment of the mounting plate, it was determined by engineering authority at Hill AFB that the wind tunnel calibration could be approved by obtaining 50 AOAT probes received directly from the manufacturer, and place each of them onto the mounting plate and ensure that they passed static friction tests. The plate was adjusted so that all probes passed calibration, and it was assumed that the alignment of the mounting plate was within the required $\pm 0.0625°$ of the free air stream. After the wind tunnel alignment plate was certified, each X-probe was again calibrated and placed on the mounting plate of the wind tunnel. An angle measurement was taken, recorded, and defined as the offset from $0°$ for each X-probe. This would then be used during calibration to offset a rotation stage and ensure that there was consistency between each X-probe reading at the wind tunnel. With this offset method, each probe could measure the alignment angle of the mounting plate to within $\pm 0.0625°$.
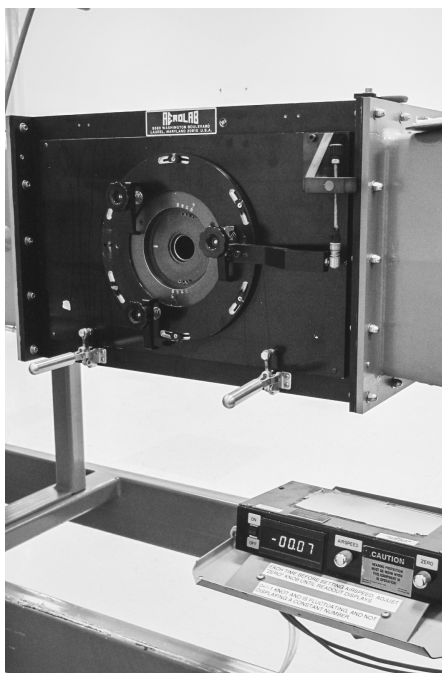
Fig. 1.4: Test section of the wind tunnel with the wind tunnel velocity indicator.

Although this method was approved as a correct calibration method by engineering authority, the actual angle of the mounting plate could not be measured and verified since this method was based on previous calibrations of AOATs from the manufacturer. Since this measurement was not directly related to a calibration standard, if the probes broke and the alignment plate was accidentally moved, the only way to again certify the angle alignment of the wind tunnel would be to repeat the process of obtaining and measuring angle readings from 50 AOATs from the manufacturer, which is a long and difficult process. Another issue that frequently occurred was that hot-film probes are extremely sensitive and the slightest bump can alter the offset recorded with a probe. If this was to happen to all of the hot-film probes, it would be impossible to trace the chain which referred back to the measurements of the 50 AOATs.

The offset method explained above was deemed a temporary fix, and a more robust method which ensured no dependency on AOATs was sought. The object of this thesis is to investigate other methods of calibration and sources of uncertainty from the hot-film X-probe anemometer. Recommendations and experiments will also be performed to ensure that future use of an X-probe anemometer in a similar application will produce confident results to other applications. A hot-wire or hot-film anemometer system can then be used as a route to achieve appropriate requirements with the knowledge gained from the results of these experiments.

1.2 Literature Review

In order to determine a solution to align the mounting plate on the wind tunnel at Hill AFB, a literature review Is presented with further information about thermal anemometers. Other possible calibration methods are also presented, demonstrating additional solutions to align the wind tunnel mounting plate according to the needed requirements.

1.2.1 Thermal Anemometers

Lekakis [2] provides a basic background of thermal anemometers that is explained here. Thermal anemometer systems use sensors made of a thin wire or quartz covered in a

conductive film and heated to a temperature of around $250°$ Celsius. A resistor, or heated wire, will have it's resistance change as it is heated up or cooled down. This means that there will be a change in resistance when the heated thermal anemometer sensor is cooled by forced convection. This sensor is placed in a Wheatstone bridge, or a circuit with resistors that are arranged so that the resistance of each side of the circuit is balanced.

A thermal anemometer can have two modes of operation. One is a Constant Current Anemometer (CCA), where the current that travels through the hot-wire or hot-film sensor remains the same. In a CCA, when the resistance changes due to the sensor being cooled, the voltage output from the anemometer circuit will also change and can be recorded. This change in voltage can be related to the velocity, and a calibration can be formed.

Another mode of operation for a thermal anemometer is constant temperature. A Constant Temperature Anemometer (CTA) is created by placing this sensor in a Wheatstone bridge with a feedback amplifier, which forces the sensor resistance and temperature to remain the same, even during cooling. Similar to a CCA, a CTA causes a change in output voltage from the Wheatstone bridge circuit which can be recorded and used to relate the voltage to a velocity. CTAs are used more often than CCAs due to their much higher frequency response to velocity measurements than CCAs [2, 3].

Thermal anemometers can have single or multiple sensors, which can be configured to fulfill a specific need as long as they are not limited by manufacturing processes. Each probe configuration has a specific purpose, and the application of the probe must be considered in order to select the appropriate sensor. Lekakis, as well as Fingerson and Freymuth [2,3], show how an X-probe is used to measure two components or dimensions of velocity, one for each sensor in the probe. Similarly, a thermal anemometer probe with three or more sensors can determine all three components of the velocity, allowing an air flow to be fully characterized in all three dimensions. However, if the flow is restricted to be purely two-dimensional, then an X-probe is sufficient to fully define the magnitude and direction of the velocity. Thus a more time consuming method of calibrating three or more sensors on one probe can be avoided.

1.2.2 Hot-film and Hot-wire Anemometers

Thermal anemometers may also be differentiated by the type of sensor. Two prominent types are hot-film and hot-wire probes. Hot-film sensors are typically thicker and made out of quartz or Pyrex and coated with a conductive material, such as platinum or nickel. Hot-film sensors are typically are between 25-50 μm in diameter compared to hot-wire sensors, which are around 4 μm in diameter which allow hot-film sensors to be stronger than hot-wire probes [2]. Because hot-film sensors are more rigid, they do not flex when a fluid flows over them. This is an important characteristic, because flexing of sensors can cause errors during measurement. Consequently, hot-films may be used in fluids which have many contaminants in them, or in dirty environments, and can also take measurements in liquids [2]. Fingerson and Freymuth [3] state that the thickness of a hot-film sensor is beneficial because it can better withstand impacts of particles and can prevent calibration drift during measurement.

An advantage of using a hot-wire probe instead of a hot-film is that the smaller size of a hot-wire probe results in a higher ratio of the length of the wire to its diameter. This is associated with a lower signal-to-noise ratio at high frequencies, increased frequency response, and spatial resolution [2]. In other words, the voltage signal received from the Wheatstone bridge may have less noise with a hot-wire than a hot-film sensor. This is an important factor to consider if a measurement needs less noise to meet requirements.

One weakness of the thinner hot-wires is that in dirty flow, dust or other small particles can attach to the sensors and change the thermal conductivity of the wire by insulating it. If the conductivity of the sensor is changed, then the rate the wire is cooled will also be affected, and the calibration between a set of voltage and velocity readings will change, causing errors during measurement [2].

The majority of the research on thermal anemometers that will be discussed is related specifically to hot-wires. However, Lakakis [2] explains that there is no difference in the calibration methods between a hot-film and a hot-wire sensor. He also states that there are no reasons why a hot-wire sensor calibration method cannot be applied to a hot-film sensor. According to Fingerson and Freymuth [3], the velocity and angle sensitivity between a hot-

wire and hot-film sensor are almost identical. Therefore, while the studies that explain the calibration methods that will be discussed mostly use hot-wires, these methods can generally be applied to hot-film sensors as well.

1.2.3 Laser Doppler Anemometry

In addition to hot-wire and hot-film anemometry, Laser Doppler Anemometry (LDA) is a widely used system for determining the velocity of turbulent or unsteady flows [2]. Fingerson and Freymuth [3] state that one of the major advantages of an LDA system is that it uses light to track the velocity and direction of particles, providing a direct measurement of the air velocity in a wind tunnel. This can be compared to a thermal anemometer, which only gives an indirect measurement of the velocity components through voltage readings from the thermal cooling of a heated wire, discussed previously.

Another advantage that LDA systems have over thermal anemometers is accuracy at very low velocities [3]. Thermal anemometers are dependent almost entirely on convective cooling, and the effects of conduction and radiation are minimal and assumed to be zero. Fingerson and Freymuth [3] state that when air cools a thermal anemometer at a low enough velocity, the heat transfer from conduction and radiation become more prominent than at higher velocities. Since most equations used during calibration of a thermal anemometer do not account for conduction or radiation, there may be large errors with hot-wire and hot-film sensors at low air speeds.

However, according to Lekakis [2], hot-wire and hot-film anemometers are often preferred instead of LDAs in many instances, due to their technical and economic merits. Additionally, Fingerson and Freymuth [3] state that LDAs generally have higher noise and cost. While good at determining the flow velocity and direction over an object inside of a wind tunnel, LDAs do not provide a direct way to align a plate mounted on the external part of a wind tunnel, such as the one at Hill AFB. In order to use an LDA for this application, another fixture must be built and attached to the alignment plate. An LDA would then need to determine the flow around that fixture and calculate the angle of the plate. Using an LDA, therefore, cannot provide a direct measurement to the mounting plate.

1.2.4   Pitot Tubes

Another method of measuring the flow angle in a wind tunnel is to use a multi-holed pitot tube. This type of probe commonly has three, five, or seven holes, with one hole in the center and the remaining holes located around it in a circular pattern. When this type of pitot tube is rotated, a slight difference in dynamic pressure is created between the holes located on opposite sides of the center hole. If the probe is aligned so that all holes are directly facing the flow, the pressure readings from ports on opposite sides of the probe will be equal, enabling the probe to provide a zero flow angle measurement. The flow angle readings of a multi-hole pitot tube, such as the ones manufactured by Aeroprobe, are calibrated to an accuracy of $\pm 1°$ [4]. This does not meet the calibration standards that are required by the Hill AFB wind tunnel.

Another type of pitot tube frequently used to measure velocity is a Kiel probe. This probe was first developed by Kiel in 1935 [5] to produce a dynamic pressure sensor that is insensitive to both pitch and yaw. It consists of a dynamic pitot tube surrounded by a venturi shaped sheath. The advantage of this design, as demonstrated in the K12 Kiel probe from Flowkinetics, is that the venturi directs the flow into the pitot port of the Kiel probe, which allows the flow to have practically no sensitivity to yaw or pitch by as much as $\pm 49°$ of the airflow [6]. Therefore, the error caused by misalignment of the probe is practically eliminated.

The dynamic pressure measured from a Kiel probe must be combined with a pressure reading from a static pitot tube to find the velocity of a flow. Although a hot-wire or hot-film X-probe sensor can be used to find both the magnitude and direction of a flow at specific point, a Kiel probe can be used to validate velocity measurements from a thermal anemometer to ensure that a proper calibration was performed.

1.2.5   Summary of Wind Tunnel Instruments

The instruments for measuring the velocity and angle of wind tunnel flow that are discussed in sections 1.2.2 - 1.2.4 are summarized in Table 1.1 and Table 1.2.

Calibration Instrument	Advantages	Disadvantages
LDA	• High accuracy at low velocities • Directly measures the flow	• Generally produces higher noise • High cost
Multi-Holed Pitot	• Initial calibration is required • Regular calibration is only required on differential pressure transducers	• Accuracy is typically $\pm 1°$
Kiel Probe	• Initial calibration is required • Regular calibration is only required on differential pressure transducers • Not sensitive to pitch or yaw by up to $\pm 49°$ for velocity measurements	• Cannot measure angle of flow, only can measure the magnitude of the velocity

Table 1.1: Comparison of various wind tunnel instruments

1.2.6 Calibration Methods for Hot-wires and Hot-films

There are many different ways to calibrate a thermal anemometer. As Fingerson and Freymuth [3] point out, no matter which calibration method is used, it is important that the conditions during calibration are repeated as closely as possible to the conditions used for measurement in the wind tunnel. In fact, they state that the accuracy of an thermal anemometer is highly dependent on how well the calibration conditions are repeated during measurement. If the orientation of the probe or the temperature of the flow is changed between calibration and measurement, there will be errors that may be difficult, if not impossible to detect.

Calibration Instrument	Advantages	Disadvantages
Hot-wire Probe	- Higher length-to-diameter ratio - Low signal-to-noise ratio - Increased frequency response - Increased spatial resolution	- Smaller diameter wires can be broken by contaminants in dirty environments - Particles can insulate wires and cause measurement errors - May flex during measurement
Hot-film Probe	- Larger diameter $(25 - 50\mu m)$ is more robust and can be used in dirty environments or liquids - Not likely to flex during measurement	- Small length-to-diameter ratio when compared to hot-wires - Typically higher noise than hot-wire probes

Table 1.2: Comparison of various wind tunnel instruments (continued)

Jorgensen's equation

One of the oldest and most common thermal calibration methods is based on the forced convection cooling of a heated cylinder developed by King [7]. Since a hot-wire or hot-film sensor can be modeled as a very small cylinder, King's research provides a natural application to the calibration of hot-wire and hot-film probes. King defined the relationship between the velocity and the output voltage from a thermal anemometer sensor by the following power law shown in Eq. (1.1).

$$V^2 = A + BU^n \qquad (1.1)$$

Where

$V =$ voltage

$U =$ velocity

$A, B, n =$ regression fit constants

This relationship, known as King's Law, allows a relatively quick calibration to be performed for a hot-wire or hot-film probe. One method using King's law is shown by Bradshaw [8]. Calibration is performed by collecting the output voltage (V) from the sensor at multiple velocities (U) at a single angle of attack, and then performing a regression fit of the data by using Eq. 1.1. This regression fit defines the values for A, B, and n, and can be used to fully characterize the velocity measurements from the hot-wire or hot-film probe. One issue with this method, according to Lueptow et al. [9] is that the model is not accurate for multiple angles. This is due to calibration being performed at one angle of attack. If Eq. 1.1 is used, the velocity components that are not directly measured can only be estimated by the cosine law shown in Eq. 1.2.

$$U_{eff} = Qcos(\beta) \tag{1.2}$$

Where,

$U_{eff} =$ effective cooling velocity

$Q =$ magnitude of velocity vector

$\beta =$ angle between vector normal to sensor and velocity vector

Using equations developed by King [7], Hinze [10], and Gilmore [11], Jorgensen [1] developed an equation which is commonly used to calibrate hot-wire and hot-film anemometers shown in Eq. (1.3).

$$U_{eff}^2 = U_N^2 + k_1^2 U_T^2 + k_2^2 U_B \tag{1.3}$$

Where,

U_{eff} = effective cooling velocity

U_N = normal velocity component

U_T = tangential velocity component

U_B = binormal velocity component

k_1 = yaw correction factor

k_2 = pitch correction factor

This equation is based on the theory of effective cooling velocityU_{eff}, or the effective cooling velocity, which is the equivalent velocity that is perpendicular to the hot-wire or hot-film sensor and gives the same voltage response as the free air stream applied to the probe during calibration [12]. U_N, U_T, and U_B are the components of the flow velocity that are normal, tangential, and bi-normal to the sensor. The terms $k_1$and k_2 are the yaw and pitch factors respectively, and account for the cooling effects in the tangential and bi-normal directions cause by the length-to-diameter ratio of the sensor, as well as the separation of flow over the prongs supporting the sensor. These correction factors can be determined by experimental data to approximate and correct these errors.

Jorgensen [1] performed his study by determining the values of k_1 and k_2 at various velocities. Results from this investigation show that if the pitch factors for the probe are neglected in turbulent flow, measurement errors between 5% to 12% can be expected, versus an error of approximately 1% to 2% when the pitch factor is included. If an assumption is made that there is no bi-normal velocity U_B acting on the probe, then Jorgensen's equation can be reduced to the two-dimensional equation found in Eq. 2.1 and Eq. 2.2. This assumption can be made when the thermal anemometer probe is oriented perpendicular to the flow at the calibrator as well as in the wind tunnel during the measurement phase. It is important to note that it is virtually impossible to orient the probe so that the bi-normal velocity is zero. Even if great care is taken to place the probe in a direction to eliminate bi-normal flow, there will still be at least a small error from this misalignment. As with any assumption, it must be decided if this error will affect the desired results. In order to

validate their significance, a standard or other method which does not use the assumption must be used to compare the results and confirm if the errors are small enough to meet the requirements.

Look-Up Table

Burattini [13] states that there are two main methods of calibrating hot-wires. One is the effective angle method, as explained by King and Jorgensen, and the other is a look-up table method. Essentially, this method measures and records the voltage of each sensor at various angles and velocities, and then uses these values to reference when measuring at a wind tunnel.

There are many advantages to using a look-up table method. One is that there are multiple ways that it can be implemented in order to fit an appropriate application. Also, this method does not have as many limitations as the effective angle method. Using a static check, Burattini [13] shows that an effective angle calibration will incorrectly reduce the range of estimate velocity components, and may provide inaccurate results at low velocities. His recommendation for a more reliable approach is to use a look-up table instead of an effective angle method.

Lueptow et al. [9] explains that an advantage of calibrating at various angles and velocities to form a look-up table is that this method does not require any assumption that the angles between the two hot-wires of the X-probe are $90°$ apart. Additionally, according to Lekakis [2] and Lueptow et al. [9], the advantage of using a look-up table method is that there are no inherent assumptions concerning the sensor cooling, and no need for a precise knowledge of probe angles. The correction factors and linearization of the output required with King's law and Jorgensen's equation also no longer need to be performed. The study made by Jorgensen, showing the errors from ignoring the pitch factor also are eliminated, since the bi-normal velocity is no longer necessary for calibration. Any errors produced by the probe not being perfectly perpendicular to the flow are therefore reduced.

There are also some disadvantages to using a look-up table calibration method. Burattini [13] states that although the look-up table allows fewer assumptions about the ori-

entation and configuration of the probe, the time it takes to acquire the needed data to produce a look-up table can be significantly higher than using an effective angle method. He compares the time of 10 minutes to calibrate with the effective angle method to 40 minutes with the look-up table method. This increase in time is due to the number of points that must be measured when compared with those of the effective angle method. For example, a look-up table calibration in the experiment that Willmarth and Bogar [14] performed with an X-wire probe needed a total of 400 calibration points as opposed to the effective angle method used at Hill AFB which uses 32.

Another constraint of the look-up table method, pointed out by Lekakis [2], is that it can be difficult to implement if the temperature of the flow fluctuates. When this happens, the cooling of the sensors will also fluctuate, and the noise from the bridge voltage readings will increase. A temperature correction factor can be applied to the voltage readings, but it can be difficult if the temperature fluctuates constantly and rapidly.

There are many variations to the look-up table method which have been developed over the years. The first recorded use of a look-up table method on an X-probe was performed by Willmarth and Bogar [14]. Another look-up table method discussed by Johnson and Eckelmann [15] used twelve partial derivatives. Although accurate, this method is complicated and time consuming due to the extremely large number of measurements that must be taken. A more efficient look-up table method was developed by Zilberman [16] in 1981, however it was not fully documented. In 1988, Lueptow et al. [9] explained Zilberman's look-up table method in greater detail. This method can be performed by placing a thermal anemometer probe in an airflow at various velocities and angles, which can then be related to the resulting Wheatstone bridge output voltage from each sensor.

The look-up table method used by Leuptow et al. to calibrate an X-probe is performed by using a range of pitch angles between $-30°$ and $30°$ instead of the full range of angles for the sensors, which would be $-45°$ to $45°$, since this is the range of operation of the sensors due to their perpendicularity [2]. This choice was based on Johnson and Eckelmann's findings that the interference of sensor supports and the tangential component of the velocity

on cooling the sensor allows a reduction in the range of measurement angles from the entire range available for an X-probe [15].

The first step when performing the method shown by Leuptow et al. [9] is to gather raw calibration data, such as bridge voltage, velocity, and angle at the lowest velocity in a set of predetermined velocities. The angle between the air stream and the X-probe can next be adjusted by rotating the probe to a set of predetermined angles, using the range between $-30°$ to $30°$. After all angle measurements are completed, the velocity of air is changed and the probe is again rotated through the set of angles needed for calibration. This process is repeated until the entire range of velocities and angles needed for calibration are applied to the hot-wire, and the bridge voltages for each sensor, E_1 and E_2, are plotted and cubic spline regression fits performed along each angle measurement. This is repeated for velocity until the calibration is completed.

This set of data can be stored in a file where it may be referenced during live measurements of E_1 and E_2 from the X-probe at the wind tunnel. Through an interpolation method, the live measurement voltage is converted to obtain a measurement of the angle (γ) and velocity (Q) of the airflow. Lueptow explains that the main source of error with this method is the interpolation method used between data points. However, if a smooth surface is formed from the data, this error is negligible. Lueptow estimates that for velocities that are less than 2.4 m/s, the maximum error for the velocity components at zero angle of attack (U) and perpendicular to zero angle of attack (V) is 1.7% and 1.9% respectively, with this error dropping to 0.3% and 0.6% when the velocity is above 2.4 m/s.

Another look-up table method is discussed by Ovink, [12] who developed a look-up inversion method from a first-order polynomial model shown in Eq. (1.4).

$$E^2 = c_0(\alpha) + c_1(\alpha)U_0^{1/2} \tag{1.4}$$

Where,

$E =$ bridge voltage

$U_0 =$ velocity

c_0, c_1 = regression fit coefficients

α = angle of attack

The value of E in this equation is the bridge voltage for each sensor in an X-probe, and c_0 and c_1 are coefficients found by the equation of each line when the values of E_1 and E_2 are plotted on the same graph. Ovink states that this method produces a relative error of 0.15%, which to justify a look-up inversion approach with the hot-film probe in order to minimize error and provide more consistency with velocity and angle measurements in a wind tunnel. This method is especially accurate and effective when purely two-dimensional flow is encountered, but as mentioned by Ovink, turbulent flows are never two-dimensional. This is an important observation to make with regards to thermal anemometers, since these types of probes are commonly utilized to measure turbulence. Ovink's study determined that hot-wire probe measurements may have as much as 25% error in velocity and its components as turbulence intensity is increased to over 50%. However, these results also showed that when there is 5% or less turbulence intensity, errors were minimal. Therefore, Ovink's point that two-dimensional turbulence can cause high errors is not a concern if the turbulence intensity is less than 5% [12].

Another look-up table method was performed by Burattini [13], employing the advantages of the griddata function in MatLab. This function allows an input of a set of data containing the bridge voltages E_1 and E_2, the velocity U, and the angle γ at each calibration point. A cubic spline option is also available with griddata, and can interpolate the data accurately. This method requires only a few lines of code to implement, and is a fast way to form a look-up table from raw calibration data.

Temperature Correction

As mentioned in section 1.2.1, the basic mechanism that allows a hot-wire or hot-film anemometer to function is the cooling of the sensor by forced convection as air blows across a heated wire or film. If the temperature of the air that cools the thermal anemometer changes during calibration, or if the temperature of air in the wind tunnel changes during

the measurement phase, a significant error in measurement can occur.

A temperature correction can be performed to ensure that any errors caused by temperature differences between the air during calibration and measurement at the wind tunnel is minimized. One method is discussed by Dijk and Nieuwstadt [17] and which TSI Incorporated [18] recommends for their products and has shown to be valid over a change in temperature of $2°$ to $3°$ Celsius between measurement and calibration is found in Eq. 1.5.

$$E_b = E_o \sqrt{\frac{T_w - T_{cal}}{T_w - T_{exp}}} \tag{1.5}$$

Where,

E_b = temperature corrected bridge voltage

E_o = measured bridge voltage

T_w = temperature of the sensor

T_{cal} = temperature of the air stream during calibration

T_{exp} = temperature of the air stream during measurement.

Benjamin and Roberts [19] found that a slightly better temperature correction can be performed by rearranging and performing a first-order Taylor expansion on the Eq. 1.5 to obtain Eq. 1.6.

$$E_b = E_o \left(1 - 0.5 \frac{T_{cal} - T_{exp}}{T_w - T_{exp}} \right)^{.55} \tag{1.6}$$

This equation was found to be effective at correcting errors due to large changes in temperature for low velocities, up to 14 m/s, or 27 knots. Ardekani and Farhani [20] also discuss a variant of Eq. 1.6 which is shown in Eq. 1.7:

$$E_b = E_o \left(\frac{T_w - T_{cal}}{T_w - T_{exp}} \right)^{.5(1 \pm m)} \tag{1.7}$$

By substituting different values of m in the above equation, Ardenkani and Farhani found that at 20 m/s, the value of m that produced the smallest error and was easiest to

implement, were values from 0.2 to 0.3.

1.3   Research Objectives

The objective of this project is to experiment with different calibration methods to create a successful calibration method that consistently meets the $\pm 0.0625°$ alignment requirement between multiple X-probes at the Hill AFB wind tunnel. In order to accomplish this accuracy, the calibration method based on Jorgensen's equation will be performed and recorded for multiple probes and compared to the look-up table calibration method. The assumptions made to perform Jorgensen's method will be evaluated and their validity discussed.

Since the biggest problem with the Hill AFB calibration method has been that it cannot show consistency between multiple probes, a modified probe support will be used so that the orientation of the probe can be adjusted by tightening set screws in the attempt to match conditions between calibration and measurement. This decision is based on the observation made by Fingerson and Freymuth [3] that conditions at calibration must match as closely as possible the conditions during measurement in order to reduce error. The modified probe support will align each of the probes so that their axes of rotation are comparable. It will also support the probe to resist any forces in the wind tunnel that may deflect it during measurement.

Utilizing the information presented in the literature review, decisions will be made in order to successfully calibrate the alignment plate on the Hill AFB wind tunnel. First, since the operating velocity during testing is never less than 50 knots, the errors from using a hot-film anemometer at low velocities will not be a concern. Implementing an LDA system for this wind tunnel would be expensive, requiring a complete redesign of the system and new fixtures that would add even more to the cost and complexity. As discussed previously, an LDA could also increase the noise in the results. Therefore, an LDA system will not be used for tests at Hill AFB. Instead, the focus will be on modifying the hot-film anemometer system to achieve the plate alignment requirements.

Another important factor to consider is that the Hill AFB wind tunnel is open-loop.
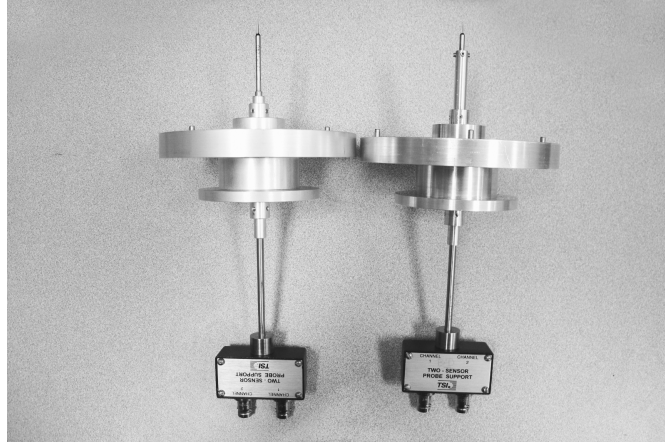
Fig. 1.5: Original and modified probe support fixtures with hot-film probes installed. The original probe support fixture is on the left, where the modified probe support is on the right.

When the wind tunnel is operated, air molecules move around the room from the outlet and back around to the inlet of the wind tunnel. This causes friction between air molecules as the air flows around the room, causing the air in the wind tunnel to warm up. This is a slow, but still apparent process. If the wind tunnel runs for more than 15 minutes, the temperature of the room may increase by as much as $0.5°$ Fahrenheit. To reduce errors during measurement from this change, a temperature correction must be implemented. The manufacturer of the X-probes used at Hill AFB, TSI [18], recommends the using Eq. 1.5 to compensate for temperature changes in the flow. This equation is widely accepted as an accurate temperature correction method.

The range of angles suggested by Lueptow et al. [9] of $-30°$ to $30°$ fully define the possible angle measurements that an X-probe can take in a wind tunnel. If an assumption is made that a range of angles less than $\pm30°$ will be encountered during measurement of the free air stream, then the angles used for calibration will also have a tighter range. As mentioned in section 1.1, the the mounting plate on the wind tunnel at Hill AFB is currently certified as being calibrated due to the measurements from 50 calibrated F-16 AOATs obtained directly from the manufacturer. The results of these measurements showed that the AOATs could all pass calibration on the Hill AFB wind tunnel, showing

that although the exact angle the plate is aligned to is not known, it is assumed to be closely aligned to the free air stream. Since the only angle measurement that is required at the Hill AFB wind tunnel is the mounting plate to be within $0.0625°$ of the free air stream, a range of angles that is close to $0°$ may be applied after there is high confidence that it has been successfully adjusted to $0°$. This will minimize the measurements and time necessary to perform the look-up table method.

A Kiel probe will be used to measure the velocity of the wind tunnel. Since the Hill AFB wind tunnel is required to be within ± 5 knots of a calibrated standard at 50, 70, 90, 110, 120, and 130 knots, these velocities will serve as measurement points for the Kiel probe. As discussed in the literature survey, the Kiel probe is an instrument that accurately measures dynamic pressure and is not sensitive to yaw and pitch angles by as much as $49°$ away from the free stream velocity. This means that even though the mounting plate may not be perfectly aligned with the air stream in the wind tunnel, it can still accurately measure velocity. To test the accuracy of the velocity measurements from the hot-film probe, the results from the Kiel probe will be compared to velocity readings from a hot-film probe.

The objective of this thesis is not only to perform a successful alignment of the mounting plate on the wind tunnel at Hill AFB, but also to provide information on how a hot-film probe performs with rotation alignments in a wind tunnel. Since there was no literature found on best practices for aligning the an object in a wind tunnel with a thermal anemometer, this information can be valuable to future applications. The results from this thesis will show if a hot-film anemometer probe can provide accurate alignments in a wind tunnel, or if other methods or equipment should be considered instead to perform this function.

CHAPTER 2

Approach

2.1 Jorgensen's Equation Method

The look-up table method as explained by Lueptow et al. [9] and Ovink [12] in the literature survey is a common calibration method for thermal anemometers. The method currently used at Hill AFB to calibrate hot-film X-probes includes Jorgensen's equation and the assumption that that the sensors of an X-film probe are perpendicular to each other. This means that the velocity component tangential to sensor 1 is equivalent to the normal component of the velocity on sensor 2. Also, the normal component of sensor 1 is equivalent to the tangential component of the velocity on sensor 2. This relationship is crucial for the current calibration method for the hot-film anemometer at Hill AFB. From this definition, Eqs. (2.1) and (2.2) can be derived.

$$U_{eff_1}^2 = U_{N1}^2 + k_{y1}^2 U_{T1}^2 \tag{2.1}$$

$$U_{eff_2}^2 = U_{N2}^2 + k_{y2}^2 U_{T2}^2 \tag{2.2}$$

Where,

U_{eff_1} = effective cooling velocity for sensor 1

U_{eff_2} = effective cooling velocity for sensor 2

U_{N1} = normal velocity component for sensor 1

U_{N2} = normal velocity component for sensor 2

U_{T1} = tangential velocity component for sensor 1

U_{T2} = tangential velocity component for sensor 2

k_{y1} = yaw correction factor for sensor 1

k_{y2} = yaw correction factor for sensor 2

It is virtually impossible for the two sensors to be exactly perpendicular to each other due to manufacturing constraints, so assuming this to be true will always result in some error. This may or may not be acceptable, depending on the size of the error as well as the required accuracy. As stated in the literature review, a look-up table method eliminates this assumption. The measured voltage, velocity, and angle measurements are all that are needed. Voltage readings from each sensor in the X-probe are recorded to form a look-up table, and a cubic spline interpolation method implemented to interpolate between voltage points in the look-up table to determine the velocity and angle measurements.

2.2   Probe Characterization

Before calibration, each hot-film probe must be characterized to find angle measurement limits. This will be accomplished by measuring the noise from the bridge voltage readings. This important step will determine the minimum angle that can accurately be measured by each X-probe. During the characterization process, the noise from the voltage measurement at 0° angle of attack cannot interfere with the next angle measurement. If it does, then there will be noise interference between the two data points for these two angles in the look-up table. This would cause a high likelihood that measurement of these angles will be indistinguishable from each other.

This check can be performed by first setting the velocity to the test velocity used at the wind tunnel, which in this case is 120 knots, and is the velocity used to test the static friction of the F-16 AOAT. The rotation stage will be set to 0° and at least 100 data points of the bridge voltage reading for each sensor will be collected. Statistical data, including the mean and standard deviation of the data also will be calculated.

Next, the rotation stage will be set to 0.0625°, followed by −0.0625°. These angles were chosen since this is the limit required for the alignment plate on the wind tunnel. Three standard deviations from the mean at 0° and ±0.0625° will quantify the noise at each of these angles. If the noise at 0° and ±0.0625° is large enough that their readings overlap,

then it is assumed that the interference at each angle will cause the angle measurements to not be distinguished from each other. If there is interference with the standard deviations between the readings at zero and $\pm0.0625°$ at 120 knots, then higher velocities will be used until either the $0.0625°$ angle reading requirement can be met, or the maximum allowable 150 knots at the calibrator is achieved. It is possible that higher velocities will reduce the amount of overlapping noise since the look-up table developed by Lueptow et al. [9] shows that as the velocity on a look-up table increases, the bridge voltage data points are further away from each other. If three standard deviations of the mean from the voltage readings at $\pm0.0625°$ still cannot be separated from three standard deviations from the mean of the data measured at $0°$ at a higher velocity, then the minimum angle that can be measured and not interfere with the noise from a measurement at $0°$ will be determined. If this angle is not less than $0.0625°$, the noise must be reduced until this is achievable. If the noise is too high and must be reduced to distinguish the voltage data between $0°$ and $\pm0.0625°$, then the data will be evaluated for possible signal conditioning techniques to reduce this noise so that the signals at different angles can be distinguishable.

This method of finding the minimum distinguishable angle measurement from $0°$ as explained above will determine the first point on the positive and negative side of $0°$ for the look-up table. If the minimum angle is greater than $\pm0.0625°$, then it will be impossible for a look-up table method to meet the requirement for the mounting plate on the wind tunnel to be aligned to within $\pm0.0625°$ of the free air stream.

If the noise measured at $\pm0.0625°$ does not interfere with the noise at $0°$, then according to the look-up table method, it should be possible to calibrate the alignment plate to within $\pm0.0625°$ of the free air stream at the wind tunnel. In order to complete this calibration, the velocity will first be set to a value on the low end of the range needed for calibration. Then, the rotation stage will be rotated to the angles $\pm0.0625°$, $\pm0.1°$, $\pm0.5°$, $\pm1.0°$, $\pm1.5°$, $\pm2.0°$, and $\pm2.5°$, and the bridge voltage for each sensor will be recorded at each point in a look-up table.

2.3 Look-up Table Approach

Since the only measurement that is of concern when aligning the mounting plate is $0°\pm0.0625°$ to the free stream velocity of the wind tunnel, the measurements that are further away from $0°$ do not need to be as accurate as those closer to $0°$. All angle measurements that are further from zero than $\pm0.0625°$ will only be used to determine which direction to rotate the plate until $0° \pm 0.0625°$ reading is achieved. This process will result in less calibration points and allow the procedure to be much faster.

After angle readings are performed at the velocity at the lowest end of the range, the airspeed will then be adjusted to the next calibration point, and the rotation stage will be set to the same angles as were with the previous velocity. This procedure will be repeated until all of the angle look-up table points have been recorded at all velocities within the range needed at the calibrator. All of the bridge voltages, velocities, and angles recorded will be inserted into the MatLab griddata function. A validation can then be made at the calibrator by adjusting to known angle and velocity settings. Voltage readings from the hot-film probe can be inserted into the MatLab griddata function, and the angle and velocity readings from the X-probe will be compared to angle and velocity readings from the rotation stage and differential pressure to ensure an accurate calibration.

The hot-film probe will then be placed onto the alignment plate on the wind tunnel, and velocity readings will be made at 50, 70, 90, 110, 120, and 130 knots by adjusting the wind tunnel velocity indicator. The velocity readings from the probe will then be compared to that of the wind tunnel. The velocity will be adjusted to 120 knots and an angle and velocity reading taken and recorded from the hot-film. A second probe will then be calibrated the same as the first probe and inserted into the wind tunnel by placing it on the alignment plate. The velocity and angle readings performed with the first probe will be repeated and recorded.

To verify the velocity measurement from the hot-film probe, a Kiel probe will be inserted into the wind tunnel at the mounting plate and velocity measurements taken at 50, 70, 90, 110, 120, and 130 knots. A K12 model Kiel probe from Flow Kinetics has been

selected for this experiment, which is not sensitive to pitch or yaw up to $\pm 49°$. This allows an accurate measurement of the velocity of the wind tunnel without needing to align the probe precisely with the free air stream. These measurements can be compared with those of the hot-film probe velocity to determine the accuracy of the calibration of the hot-film probes.

2.4 Modified Probe Support

As stated in the literature review, the accuracy of the look-up table method is dependent on the hot-film undergoing purely two-dimensional flow [12]. The current calibration method at Hill AFB has no requirements to ensure that the hot-film probe is perpendicular to the flow at the calibrator. Because of this, perpendicularity between the hot-film probes and the flow is not verified. A simple way to measure the axis of the probe being aligned with the rotation stage can be performed by inserting the probe into the rotation stage at the calibrator, and then placing a dial indicator on the support of the probe, as close to the sensors as possible without touching to avoid damaging them. Next, the rotation stage will be turned $360°$ and the misalignment of the axis of the probe to the rotation stage can be measured.

This test has been previously performed with the system at Hill AFB, and measurements from a dial indicator showed that the probe is not aligned to the axis of the rotation stage. Although these measurements were not recorded at the time, this is a problem that needs to be addressed. This is confirmed by the comments made by Jorgensen [1] and Ovink [12] about the effects on measurements when three-dimensional flow occurs, but two-dimensional flow is assumed. By ensuring that the calibrator mimics the conditions at the wind tunnel, errors will be minimized and consistency between measurement with various probes can be accomplished.

During calibration, the Hill AFB hot-film anemometer is placed in a calibrator where an air stream with a known velocity and direction is forced over the sensors at the tip of the probe. This allows minimum aerodynamic forces to be applied to the smallest section of probe possible which minimizes deformation during calibration. However, when the hot-film

probe is placed in a wind tunnel, it is subjected to drag forces along the entire length of the probe, not just at the tip. The air stream in the wind tunnel can then deform the probe similar to a circular cantilever beam. In order to determine how the lack of shielding from the air stream in the wind tunnel affects measurements, a modified probe support will be used for each hot-film probe. The support is designed with set screws that will allow the tip of the probe to be aligned with the axis of the rotation stage at the calibrator by using a dial indicator. Since the look-up table method uses only measured values and does not assume the flow direction over each sensor like the calibration method using Jorgensen's equation does, flow disturbances caused by the redesigned probe support fixture will not affect the measurements of the hot-film probe. However, to minimize the effect of aerodynamic forces caused by this new probe support fixture, the design will place the tip of the support fixture as far away as possible from the hot-film sensors, while still providing the support needed.
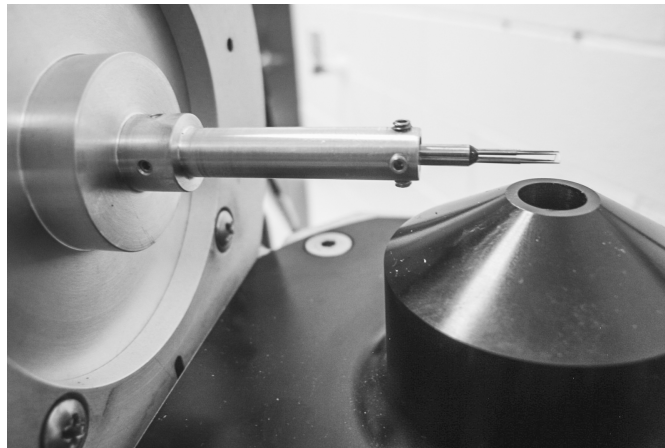
Fig. 2.1: Modified probe support at calibrator. Set screws which both hold and align the probe can be seen.

If the drag forces on the probe in the wind tunnel are significantly different than at the calibrator, then multiple effects could occur. First, the deflection of the probe will be greater at higher velocities due to the drag forces on the probe increasing. This deformation will cause a change in the direction of flow over the sensors as the velocity of the wind tunnel is increased. Instead of being purely two-dimensional flow, the probe would undergo three-

dimensional flow as it is deflected. The direction of flow over the sensors in the wind tunnel than what is produced at the calibrator, especially at higher velocities. This will a change the measurement of the probe will change from two-dimensional to three-dimensional, which means that conditions at the wind tunnel and the calibrator are no longer consistent.

The modified probe support fixture will be designed to shield the the probe from the drag forces at the wind tunnel. Results from testing with the modified as well as original probe support fixture will be compared to show the effects that drag forces have on the measurements from the probe. If there is no difference in accuracy between the results when using the modified versus original probe support fixtures, then it will be assumed that the deflection at the wind tunnel due to drag is not what is causing measurement differences between multiple probes. Instead, some other factor must be affecting the difference in angle measurements between various probes. A final summary of these studies will then be discussed and the results will be used to show the limitations and also the capabilities of this hot-film anemometer system.

CHAPTER 3

Hill AFB Configuration

3.1   Hill AFB Wind Tunnel Calibration System

The wind tunnel calibration system at Hill AFB consists of multiple pieces of equipment for velocity calibration of the wind tunnel and angle alignment of the mounting plate for AOATs. The major components of this system are described in this section, as well as any justifications for using this equipment.

This system uses a thermal anemometer to complete the calibration of an alignment plate that aligns F-16 AOATs with the free air stream in the wind tunnel. Since this wind tunnel is not located in a clean room, there is a possibility of particles contaminating the flow. In order to reduce reading errors and damage to the probe, a hot-film anemometer has been chosen instead of a hot-wire. Although a hot-wire probe would generally produce less noise and allow more accurate measurements, there was fear that using a hot-wire probe would regularly break and reading errors would occur due to particle contamination.

Since the calibration requirements are to measure and set both the direction and magnitude of the air velocity in the wind tunnel with respect to the alignment plate, a probe with at least two sensors must be used. With these requirements, the TSI 1240-20 probe, a hot-film X-probe, was chosen for the procedure. The TSI 1240-20 is a cross-flow probe, meaning that when it is used, the air flow needs to be in the same plane as the two sensors, and normal to the probe itself. Therefore, in order to take measurements with this probe, it must be oriented so that the probe is perpendicular to the flow. The TSI 1240-T1.5 is similar to the TSI 1240-20 in that it is also a cross-flow X-probe, however, it is a hot-wire instead of a hot-film probe. Hill AFB has two TSI 1240-T1.5 probes that are available for use with the calibration system if desired. They are rarely used, however, due to their extreme fragility and other disadvantages mentioned previously.

Fig. 3.1: TSI 1240-20 hot-film X-probe installed on the modified probe support on the calibrator

The TSI 1240-20 and TSI 1240-T1.5 plug into a probe support, the TSI 1155, which holds the X-probe and has two BNC connectors, one for each sensor, that can be connected via BNC cables to the other parts of the anemometer system in order to obtain voltage measurements. Since angle is a crucial requirement, a probe support fixture was also developed to hold the TSI 1155 and also fit onto the alignment plate where the AOATs are mounted. The TSI 1155 can be seen in Fig. 1.5 which shows the TSI 1155 installed in both the original and modified probe support fixtures. This modified probe support fixture was designed from drawings for the F-16 AOAT, with the dimensions and tolerances for the alignment dowel pins on the probe support matching those of the pins on the F-16 AOAT. This ensured that the form and fit of the probe support fixture was the same as the F-16 AOAT probe and would properly simulate the flow over the AOAT when in the wind tunnel.

A rotation stage was selected which had the accuracy required to meet the angle alignment requirement and to act as the calibration standard for the X-probe. Using ANSI/NCSL Z540.3, which is the same standard used to give the requirements for the accuracy of the wind tunnel plate alignment, each component of the anemometer system was determined. ANSI/NCSL Z540.3 states that a calibration is considered acceptable if the consumer risk, or risk of having a false acceptance on an instrument, is 2% or less. Alternatively, if a 2% risk cannot be proved, ANSI/NCSL Z540.3 says that the Test Uncertainty Ratio (TUR) of

the equipment can be acceptable if it is determined to be 0.25 or less, based on previous standards that were replaced by ANSI/NCSL Z540.3.

According to the TUR conditions of ANSI/NCSL Z540.3, the wind tunnel must be able to measure at least four times more accurately than the requirement of the Units Under Test (UUTs) that are calibrated on it. The alignment plate must then be within $\pm 0.0625°$ of the free air stream in the wind tunnel. Similarly, the rotation stage must be calibrated to be within $\pm 0.015625°$ of a calibration standard. To achieve this requirement, the Aerotech AGR 150 was chosen which has an accuracy of ± 20 arc-seconds, or $\pm 0.0055°$.
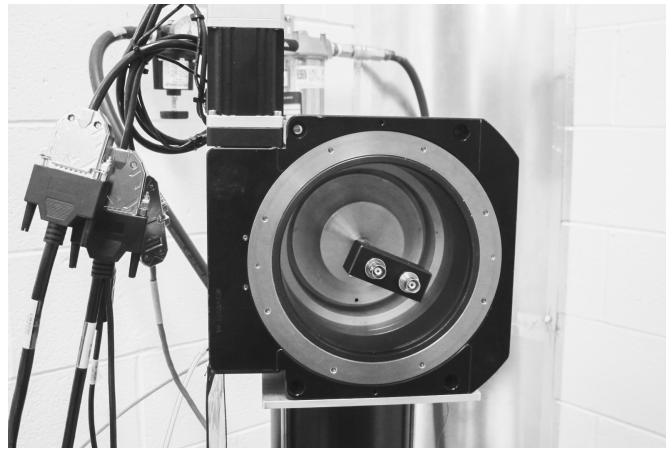
Fig. 3.2: AGR 150 rotation stage on the calibrator with TSI 1155 installed with the new probe support fixture

During the requirement definition phase of the wind tunnel, the engineering authority determined that the accuracy of the hot-film X-probe must be calibrated to within $\pm 0.0625°$ of the angle measured by the rotation stage. It was also decided that the plate on the wind tunnel needed to be aligned to within $\pm 0.0625°$ of the angle measurement from the hot-film probe. This decision was made because it was deemed that the plate itself did not give a measurement, but was aligned with an instrument that had an accuracy of $\pm 0.0625°$. With these arguments being accepted, the requirement for the angle calibration of the hot-film X-probe was defined to be within $0.0625°$ of the rotation stage.

The probe support fixture is installed onto the rotation stage via mounting plate. This

plate was designed to match the mounting holes on the alignment plate on the wind tunnel to ensure accuracy and consistency during probe calibration. The mounting plate must be aligned so that the air flow from the calibrator matches the direction of the flow when the probe is mounted to the wind tunnel alignment plate. In order to ensure accurate alignment, the mounting plate on the rotation stage has a hole that lines up with a slot at the center of the air nozzle on the calibrator where the jet of air exits when an air stream is applied to the probe. The mounting plate also contains alignment holes at $0°$, $180°$, $99.8317°$, and $-99.8317°$ which matches up with the slot on the calibrator when the rotation stage is set to each of these angles. The largest go/no go gauge that can fit through each hole and the slot at the calibrator is then found and placed through the hole at each of these angles. It is then recorded if the gauge is aligned with the slot on the calibrator, ensuring that the exit nozzle lined up correctly with the rotation stage. The stage is rotated at $0.01°$ increments clockwise and counter-clockwise until the go/no go gauge no longer fits into both the hole on the mounting plate and the slot on the calibrator. The results are then observed, and the midpoint of the offsets where the gauge successfully passes through the mounting plate hole and the calibrator slot for every angle is used to set the zero alignment of the rotation stage.

Another important part of the anemometer system is the equipment used to collect the data. One resistor of the Wheatstone bridge of the thermal anemometer system is the sensor, while the remaining resistors in the Wheatstone bridge are placed in an instrument, such as the IFA 300 produced by TSI. The IFA 300 is a CTA that also contains multiple channels to receive information from other equipment, such as a differential pressure transducer as well as a thermocouple during calibration and measurement.

In order to interpret signals from the channels of the IFA, a Data Acquisition or DAQ board converts the signals from an analog signal to a digital one. The DAQ board used with this anemometer system is a National Instruments 16 bit USB-6351 which is capable of an accuracy less than ±0.47 mV. The voltage signals from the IFA 300 are passed to the USB-6351, which converts the analog signals to digital, and sends them to a computer. The

computer then displays the voltage readings to the user though a LabView program.

To accurately determine the velocity reading during calibration, a differential pressure transducer measures the pressure from the calibrator. The equipment that conducts these measurements is the model 220DD-00100A2B that is produced by MKS Instruments. Before each calibration, this differential pressure transducer is connected to an Agilent model 34401A Digital Multi-Meter (DMM). This DMM is calibrated to an accuracy of $\pm 0.0035\%$ with a range of 12 Volts DC. At ambient room pressure, the zero potentiometer on the differential pressure transducer is set as close as possible to a zero volts measurement, with the DMM reading 0 ± 0.25 mV. This initializes the readings from the pressure transducer at zero velocity.
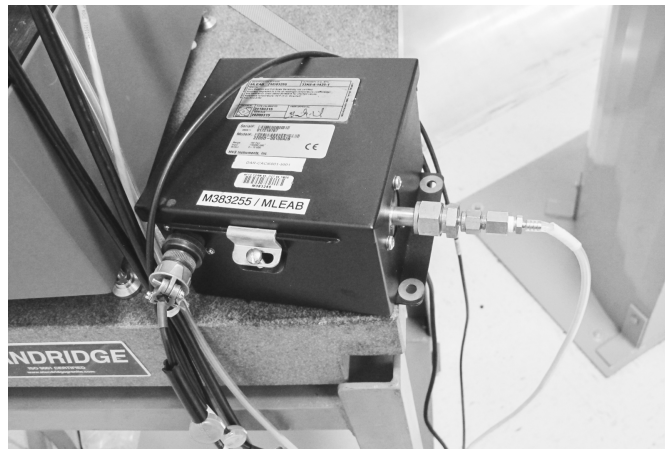
Fig. 3.3: Model 220DD-00100A2B differential pressure transducer which is used to reference the velocity during calibration of the hot-film X-probe.

The wind tunnel used for the AOAT calibration is a horizontal open loop wind tunnel, built by Aerolab with a 12x12 inch test section and a maximum velocity of 150 knots. To control the wind speed in the test section, the wind tunnel has a velocity indicator that is connected to a Variable-Frequency Drive (VFD) which controls the speed of the wind tunnel motor, and thus the velocity in the test section of the wind tunnel. The indicator is connected by hoses to both the inlet and test section of the wind tunnel in order to measure a pressure difference and determine a velocity measurement. To ensure that the wind tunnel

velocity indicator is calibrated correctly, the hot-film X-probe measures the velocity at the wind tunnel at 50, 70, 90, 110, 120, and 130 knots. These velocity measurements from the X-probe are compared to the reading from the wind tunnel velocity indicator. If the velocities do not read within ±5 knots, a zero potentiometer in the wind tunnel velocity indicator is adjusted until the readings are within ±5 knots of each other.
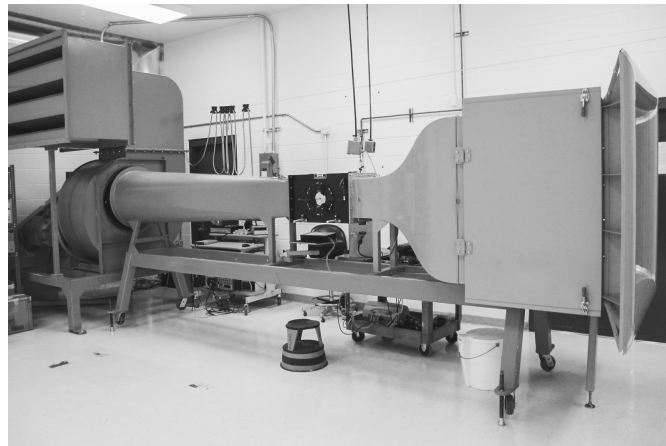
Fig. 3.4: Aerolab horizontal wind tunnel with 12x12 inch test section.

Turbulence in the wind tunnel is also a major concern, and was studied and evaluated by a contractor for this wind tunnel. As a result of this study, the inlet of the wind tunnel was modified to include a 3.5 inch wide honeycomb screen with each honeycomb being 3/8 inch wide that was placed closest to the outlet. After the honeycomb, sizes 28, 36, 42, and 20 mesh were also placed in the inlet section to aid in reducing turbulence.

Before a thermal anemometer can be used for measurement in a wind tunnel, it must be calibrated to a known set of velocities and if more than one sensor is used, a known set of angles. This can be performed by placing the probe in a calibrator where the fluid velocity can be determined by using a calibrated differential pressure transducer and rotation stage to determine the velocity of the flow, as well as the orientation of the probe during calibration.

This calibrator consists of various components that allow calibration to be performed. First, an air tube is inserted from an air source which is regulated to 30 psi. There is also a hole near the top of the calibrator's cylinder where the differential pressure transducer

can be connected for measuring the velocity of the air. The differential pressure transducer is then connected to the IFA 300 via BNC for data collection. An additional small hole allows a thermocouple to be placed to measure the air temperature during calibration. This allows temperature corrections to be performed during measurement of the air velocity in the wind tunnel. The calibrator also contains two knobs, one for larger velocity adjustment and the other for fine tuning the velocity. They control the velocity of the jet of air exiting the calibrator. Using both of the knobs and the readout from the differential pressure transducer, the velocity of the airspeed in the calibrator can be determined.
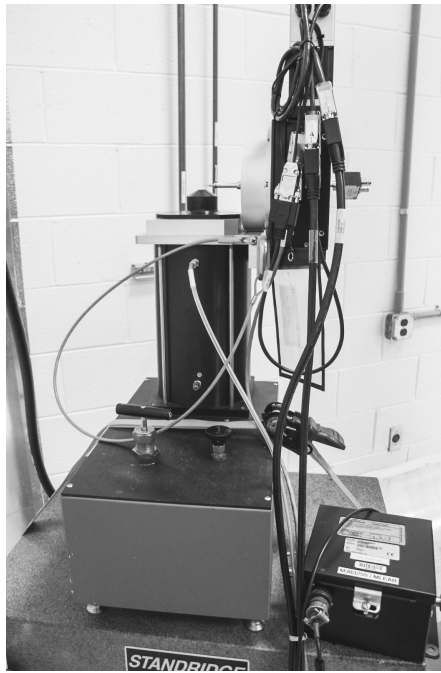
Fig. 3.5: Calibrator for the X-probe with the rotation stage and differential pressure transducer.

The top of the calibrator has a venturi nozzle where the flow exits. The hot-film probe is centered over the venturi nozzle to obtain velocity measurements. CACI modified this design by placing a plate under the venturi nozzle in order to connect the rotation stage. The jet of air coming out of the venturi nozzle simulates the air flow in the wind tunnel test section in order to calibrate the hot-film probe. To calibrate the X-probe, the rotation

stage is first positioned so that the angle of attack is zero, then the velocity of the air from the calibrator can be adjusted to a predetermined velocity. The resulting bridge voltages are then recorded and paired with the velocity from the calibrator, which is determined from the differential pressure transducer.

A predetermined set of air velocities can then be applied to the sensors, followed by the rotation of the probe to a predetermined set of angles. The resulting bridge voltages can then be recorded and a calibration table formed for later measurement in flows where the velocity and direction of the flow is unknown.

3.2   X-probe Calibration Method

As presented in the literature survey, there are many calibration methods that can be utilized to relate velocity and angles to the voltage readings from an X-probe. One method discussed previously and frequently employed is based on Jorgensen's equation. The velocity vector of the air that flows over a thermal anemometer probe can be broken into three components, one tangential to, or along, the sensor, one normal to the sensor, and one perpendicular to the sensor and parallel to the probe, also known as a bi-normal component.

Jorgensen determined that due to the separation of flow over the prongs supporting the hot-film or hot-wire sensors, as well as other variations in the probe during manufacturing, the bi-normal and tangential components of the velocity in three-dimensional flow must each be corrected by using yaw and pitch factors or high errors will result. He defined this equation as shown in Eq. (1.3).

When an X-probe is used, only two components of the flow velocity can be measured, meaning that if Jorgensen's equations are used, one component of the flow velocity must be eliminated. If it is assumed that the sensor will only undergo flow that is in the same plane as the two wires, or perpendicular to the axis of the X-probe, then the bi-normal velocity component, U_B in Eq. (1.3) can be eliminated. This assumption of two-dimensional flow then enables the use of the following procedure developed by TSI and CACI for calibration.

First, by redefining the yaw factor for each sensor in an X-probe as k_1 and k_2 for sensor

1 and sensor 2, respectively, Eqs. (2.1) and (2.2) can be formed to represent the effective velocity for each sensor in two dimensional flow [21]. These equations are the basis for the calibration of the hot-film probe used to calibration this wind tunnel system.

During the first phase of calibration, the yaw correction coefficients, k_{y1} and k_{y2} in (2.1) and (2.2) are assumed to be 0.2. Also, the X-probe is oriented so that the flow bisects the angle between the two sensors, which, due to the orthogonality assumption, means that the flow vector is $45°$ from each sensor and is defined as being $0°$ angle of attack with the sensor.

If it is assumed that the two sensors of the X-probe are orthogonal, the velocities U_{N1} and U_{T2}, as well as U_{N2} and U_{T1} can be assumed to be equivalent. The known velocity from the calibrator can then be related to U_{N1}, U_{T2}, U_{N2}, and U_{T1} by assuming that air is bisecting the angle between the two sensors of the X-probe. The velocity vector can then be transposed into the coordinate frames defined by U_{N1} and U_{T1} as well as U_{N2} and U_{T2}. If the assumptions that the two sensors are perpendicular, as well as the air bisecting both sensors are made, then Eqs. (3.1) and (3.2) can be used.

$$U_{T1} = U_{N2} = U\frac{\sqrt{2}}{2} \tag{3.1}$$

$$U_{T2} = U_{N1} = U\frac{\sqrt{2}}{2} \tag{3.2}$$

Where,

U = velocity magnitude

If the values of k_{y1} and k_{y2} are assumed to be 0.2 as is recommended by the manufacturer for this part of the calibration, the terms for U_{eff_1} and U_{eff_2} can be solved by using Eqs. (??) and (??). U_{eff_1} and U_{eff_2} can then be related to the recorded bridge voltages, relating these two values at all set velocities.

The procedure for recording the measured velocity to the associated bridge voltages is

then repeated, but instead, the velocity from the calibrator remains constant and the angle of the probe is changed by adjusting the rotation stage. The velocity chosen for this part of testing is based on the requirement for the wind tunnel. For the given wind tunnel, the airspeed of 120 knots is chosen, since that is one of the velocities from which the static friction for the F-16 is determined. While remaining at this velocity, the angle of attack of the probe is adjusted to a predetermined set of angles to find yaw response of the probe. The resulting bridge voltages are then paired with each angle measurement from which they were taken. Using the known angle of attack, α, the components of velocity in the sensor coordinate frame can be defined by Eqs. (3.3) and (3.4). The yaw factors for each sensor can also be found through Eqs. (3.5) and (3.6).

$$U_{T2} = U_{N1} = U\frac{cos\alpha - sin\alpha}{\sqrt{2}} \tag{3.3}$$

$$U_{N2} = U_{T1} = U\frac{cos\alpha + sin\alpha}{\sqrt{2}} \tag{3.4}$$

$$k_{y1}^2 = \frac{U_{eff_1}^2 - U_{N1}^2}{U_{T1}^2} \tag{3.5}$$

$$k_{y2}^2 = \frac{U_{eff_2}^2 - U_{T1}^2}{U_{N1}^2} \tag{3.6}$$

The yaw factors are related to each effective cooling velocity found in the first part of the calibration. A live measurement can then be taken by referencing the table of yaw factors relating to effective cooling for each sensor. This measurement is made by implementing Eqs. (3.7) and (3.8) to find the components of the velocity in the sensor coordinate frame. The magnitude of the velocity components in the coordinate frame of each sensor can be rotated back into the calibrator coordinate system through Eqs. (3.9), (3.10), and (3.11), where the velocity directly out of the calibrator is defined as U, where u and v are the two components of U. The angle of the flow α is also defined in Eq. (3.12) and is $0°$ when the flow is bisecting the angle between the two sensors of the X-probe.

$$U_{T2} = U_{N1} = \sqrt{\frac{U_{eff_1}^2 - k_{y1}^2 U_{eff_2}^2}{1 - k_{y1}^2 k_{y2}^2}} \qquad (3.7)$$

$$U_{N2} = U_{T1} = \sqrt{\frac{U_{eff_2}^2 - k_{y2}^2 U_{eff_1}^2}{1 - k_{y1}^2 k_{y2}^2}} \qquad (3.8)$$

$$u = \frac{U_{T1} + U_{N1}}{\sqrt{2}} \qquad (3.9)$$

$$v = \frac{U_{T1} - U_{N1}}{\sqrt{2}} \qquad (3.10)$$

$$U = \sqrt{u^2 + v^2} \qquad (3.11)$$

$$\alpha = tan^{-1}\frac{v}{u} \qquad (3.12)$$

Where,

u = velocity component orthogonal to primary axis

v = velocity component in primary axis

Most of the assumptions that are made when applying this method can produce errors that are difficult, if not impossible to account for. First, the assumption of the orthogonality between the probe's sensors is rarely, if ever true. If a probe is placed under a microscope with an instrument that can accurately measure angles, then it is possible to find the angle between the two sensors. With the current Air Force wind tunnel calibration method, the probes are assumed to be normal to each other, without being verified by measuring. This is due to the lack of equipment able to perform this measurement. If the angle between the sensors is large enough, a measurement error will result.

Second, the probe is assumed to be oriented in a direction that eliminates any bi-normal flow on the sensor. This component of velocity is defined as being along the axis of the probe

that supports the sensors, and perpendicular to the tangential and normal velocities. This assumption is important because it eliminates the bi-normal velocity term in Jorgensen's three-dimensional equation, by allowing the pitch factor to be eliminated. However, the current calibration process never checks to see if this alignment is true. A quick check was performed on multiple probes to see if the axis of rotation of the probe was aligned with the axis of rotation of the rotation stage by placing a dial indicator near the prong supports of the sensors. The measurements showed not only that it was not aligned, but the support of the probe was so weak, that a simple measurement from the dial indicator would physically move the probe and change the measurement. After investigating the probe support fixture containing the hot-film probe and probe support, it was found that the probe support fixture does not actually hold onto the probe at all, but only to the TSI 1155 probe support.

The TSI 1155 probe support allows four wires from the probe to be plugged into it that are each approximately 0.40 inches long. When the dial indicator applies pressure to the probe, the plug wires bend slightly and remain in that orientation, causing a realignment of the probe. Therefore, with not much force, the probe can be adjusted and the alignment changed.

The X-probe is calibrated with a small jet of air covering just the tip around the sensors. However, when placed in the wind tunnel for measurement, there is wind pressure acting on the entire length of the probe. With the X-probe not being fully supported and the connection wires being flexible enough to allow the probe to move under slight pressure, it can be seen that this change of force on the probe can cause problems.

By using a simple drag force formula, the difference of force applied to the probe between calibration and measurement can be estimated. Using the drag force equation shown in Eq. (3.13), the forces acting on the probe when placed in the wind tunnel can be found. In order to use this equation, the following assumptions are made:

1. The X-probe has a smooth surface

2. The air in the wind tunnel has steady flow

3. The flow is normal to probe

4. Turbulence is negligible, so it is not accounted for

Since the jet of air from the calibrator only covers the tip of the probe during calibration, it is assumed that the drag forces during calibration are minimal. Since the X-probe is a cylinder, the approximate C_D value can be assumed to be .9 according to the estimate given in Fluid Mechanics Fundamentals and Applications [22]. This estimate is obtained by first calculating the Reynolds number with Eq. (3.14) with the density of air, ρ, as measured from the pressure readings of the test section with a Kiel probe and static pitot tube, by using Eq. (3.15).

$$F_D = C_D A \frac{\rho V^2}{2} \tag{3.13}$$

Where,

F_D = force of drag

C_D = coefficient of drag

A = the cross-sectional area of the probe

ρ = density of the air

V = velocity of the airflow

$$Re = \frac{\rho V D}{\mu} \tag{3.14}$$

Where,

Re = Reynolds number

D = diameter of probe

μ = dynamic viscosity of the air

$$\rho = \frac{P_{abs} + \Delta P}{R\left(T + 273.15\right)} kg/m^3 \qquad (3.15)$$

Where,

P_{abs} = absolute pressure in test section

ΔP = Kiel pressure differential

R = gas constant

T = air flow temperature

In Eq. (3.15), P_{abs} is the absolute pressure inside of the test section of the wind tunnel and ΔP is the pressure difference reading between the static pitot tube and the total pressure reading from the Kiel probe. R is the gas constant, $287.023\ joule/kg \cdot Kelvin$ for air and T is the temperature of the flow in the wind tunnel test section. The velocity of the flow, V is defined as 120 knots, since this is the velocity from which the angle reading is taken in the wind tunnel. With these values, the density of the air in the test section of the wind tunnel can be found to be $0.0612\ lbm/ft^2$. The dynamic viscosity, μ, is defined as $1.230 \times 10^{-5} lbm/ft \cdot s$ [22]. With the same 120 knots test velocity and the cross sectional area of the probe with 0.125 inches diameter and 1.57 inches long, the Reynolds number can be calculated to be 10480.5. By using the average drag coefficient of 0.9 as previously discussed, the drag force on the cylinder can be calculated.

After finding the Reynold's number, next the drag force equation in Eq. (3.13) is applied and the force of drag can be found to be approximately 1.5 lbs. This means that that probe experiences an additional 1.5 lbs when placed in the wind tunnel versus when it is being calibrated. With the plug wires being so small and easily moved, it is possible for this small amount of force to change the direction of the probe in the wind tunnel. Therefore, the conditions during calibration could be drastically different than when measurements are taken at the wind tunnel.

This shows that a new support fixture needs to be produced that allows the user to adjust the orientation of the probe so that it will be aligned with the rotation stage during

calibration. Also, the support fixture needs to be strong enough so that the probe can withstand forces that may cause deflections during measurement at the wind tunnel.

Another assumption that could cause error in measurement with the method based on Jorgensen's equation, is that the jet of air during calibration bisects the angle between the two sensors of the X-probe. The instructions to set up the probe do not explain a measurable method to ensure that this assumption is valid. According to the instructions, the probe is supposed to be placed so that the jet of air during calibration approximately bisects the angle between the two sensors. This assumption is important because it allows the derivation of equations to transpose the velocity vector into the coordinate frame for the sensors. If this were true, it would be a simple trigonometric procedure as explained above. Because this is not true, this will produce an error that is unknown, since it is not accounted for. In order to minimize or eliminate these errors, the assumptions themselves need to be eliminated by using a different method.

3.3   Look-Up Table

A look-up table common calibration method for X-probes. As discussed in Chapter (1), this method involves placing an X-probe in a calibrator and adjusting the velocity. The angle of the X-probe is then adjusted to multiple predetermined angles, and the voltage reading from each sensor of the X-probe is recorded. The velocity of the calibrator is then adjusted to the next value in the look-up table, and the angle adjustments are repeated until the entire range of velocities and angles needed for measurement are obtained. This method has been shown to be accurate since it relies only on measurement voltages, rather than interpreting the voltages and applying them to multiple different equations. Essentially, the data collected forms, as it's name suggests, a look-up table, that can be referenced during the measurement phase.

One reason why this method would not be viable in certain circumstances is because it requires many measurements. If a total of twenty velocity and twenty angle measurements were made during calibration, this would mean that 400 total measurements would be required to obtain a full calibration. This can take more than four times longer than

using the method based on Jorgensen's equations, and may be an important factor when choosing a calibration method. However, the calibration method for the wind tunnel at Hill AFB is not performed often. After an alignment of the mounting plate on the wind tunnel is performed, another calibration does not need to be conducted until 6 months to a year later. The requirement with this calibration method is that the alignment accuracy is within $\pm 0.0625°$ of the free air stream in the wind tunnel test section. The length of calibration is still a consideration that needs to be made with a look-up table method, and is discussed in Chapter (4).

The major advantage to a look-up table method is that almost all of the assumptions needed when using Jorgensen's method are no longer required. [2, 9]This method takes raw voltage readings from the Wheatstone bridge of each sensor on the X-probe, and compares those readings to a calibration standard for velocity and angle. When the sensors on the probe encounter the exact same conditions of velocity and angle in the wind tunnel that were simulated during the calibration stage, then the reading will be identical. This means that all assumptions about the geometry and orientation of the probe are no longer needed. The one thing that does need to be ensured is that the conditions during calibration will match the conditions at the wind tunnel as closely as possible [3]. This is one of the sources of error when using a look-up table method.

The other source of error from a look-up table method is from the interpolation. In order to reduce the number of points required during calibration, the data points are interpolated to fill in the information between test points. If the surface formed by the data collected is smooth, a cubic spline interpolation method can be used with minimal error. A look-up table method with a MatLab cubic spline function will be implemented for experimentation.

3.4   Consistency

An important requirement of the probe support fixture design for the hot-film X-probe is to ensure that the conditions during calibration are the same as those during measurement at the wind tunnel. Freymuth and Fingerson [3] have stressed the need for

consistency between calibration and measurement in order to have high accuracy with a thermal anemometer. One vital aspect of this is that the probe orientation is the same during both calibration and measurement. As discussed in section 2.4, this is not accounted for in the current configuration, and therefore, must be addressed.

Another assumption is that the flow in the wind tunnel, as well as at the calibrator is two-dimensional flow, however, the probe must be aligned in order to validate that assumption. As previously discussed, the support of the probe is such that the only thing holding it in place are the four wires that plug the probe into the probe support. This makes the probe very flexible and causes the orientation of the probe to be easily changed.

In order to ensure that the orientation of the probe remains the same during measurement as well as during calibration, the design of the probe support fixture was altered. This new design lengthened part of the probe support fixture so that most of the probe would be covered, protecting it from air flow that would deflect it. Four nylon tipped set screws were also placed near the end of the probe in order to provide support and align the rotation axis of the probe with that of the rotation stage.

Alignment of the probe was performed by installing it on the rotation stage, and placing a dial indicator near, but not touching, the prong supports of the probe. The rotation stage was then rotated $360°$, while watching the dial indicator to ensure axial alignment. If the dial indicator measured greater than ±0.0005 inches, then an adjustment was made with the set screws on the probe until the dial indicator reading achieved this specification.

CHAPTER 4

Testing

4.1 Testing Setup

The equipment that was used for the testing explained in this chapter is described in Chapter (3). In addition to the equipment, four hot-film X-probes, model TSI 1240-20, and two hot-wire X-probes, model TSI 1240-T1.5, were used for these experiments. These probes are so fragile that the slightest touch on the sensors will break them. Since many hours of testing needed to be performed with these probes, it was important to have multiple probes as alternates in case any were damaged or broken.

In order to capture the readings for bridge voltage, velocity, and angle, a LabView program was developed by CACI and installed on a computer as an interface between the operator and the equipment. The outputs for bridge voltage and velocity are calculated from readings from the National Instruments DAQ board, and fed into the computer to the LabView program. Each reading from the DAQ is obtained and the average of the measurements are calculated every 0.70 seconds. This data is also averaged every ten data points to create a rolling average of the data as it is read. This rolling average aides in reducing random noise and decreases the uncertainty of the readings.

There are three modes in this LabView program that aid in the calibration process. Since the results from each of these programs will be discussed, each mode will be explained. The first is calibration mode, which initializes the IFA 300 as well as zeros the differential pressure transducer and steps through various set velocities and angles needed for calibration. The bridge voltages and differential readings at each velocity and angle are recorded in a text file to develop the calibration of the data, which is then processed using the method based on Jorgensen's equations in Chapter (3).

The next mode in the calibration program validates the calibration of the hot-film or

hot-wire probe. In this mode, the data captured in the program's calibration mode shows readings for angle and velocity that are interpreted from the bridge voltage readings of the hot-film or hot-wire probe. Readings directly from the rotation stage and the velocity calculated from the differential pressure transducer are also displayed on the computer screen. The user can then compare the angle readout from the rotation stage as well as the velocity reading from the differential pressure to the angle and velocity measured by the probe. This allows the user to validate the calibration and meet the requirements of the probe to measure within $\pm 0.0625°$ of the rotation stage at $0°$, as well as ± 1 knot of the velocity readout from the differential pressure transducer at 50, 70, 90,110, 120, and 130 knots.

The last mode of operation on this LabView program measures the velocity and direction of the air on the probe when installed on the alignment plate of the wind tunnel. This last program is used during the calibration and alignment process at the wind tunnel. The computer displays the velocity and angle readouts from the X-probe. If the angle reading is greater than $\pm 0.0625°$, then the alignment plate on the wind tunnel can be rotated until the reading is less than $\pm 0.0625°$. The velocity reading from the probe is compared to the readout from the wind tunnel velocity indicator at $50, 70, 90, 110, 120,$ and 130 knots. If the probe differs from the wind tunnel velocity indicator by greater than ± 5 knots at any of these velocities, a potentiometer on the velocity indicator is adjusted until the two agree with each other within ± 5 knots.

The calibration mode in this program was modified by CACI specifically for these tests to allow bridge voltage and angle readings to be obtained at any angle or velocity. A "write" button was also added to allow recording of the data to a text file. An accompanying MatLab file was also created to read this text file and store this data to be used for a look-up table method, and also allow the data being collected to be interpreted as needed.

4.2 Probe Characterization

Before calibration, each probe must be characterized to determine the limits of each one by finding the minimum detectable angle readings. This can be performed by a simple

measurement of the minimum unique voltage readings for each probe which will determine the noise and uncertainty of the voltage measurement for each sensor. The results shown by Lueptow et al. [9], as well as Ovink [12], show a general trend of X-probe bridge voltage readings of E_1 and E_2 become further apart between angle measurements as the velocity increases. If this is assumed as the general trend for all X-probes, then it can also be assumed that the voltage readings between two angles will be more likely to interfere with each other at lower velocities than at higher velocities.

This characterization test will discover the minimum detectable angle readings for each probe at multiple velocities and help determine the best velocities and angle measurements for the look-up table method. In order to meet the requirements at Hill AFB, the minimum angle between two voltages readings that do not overlap in measurement due to noise must be at least $0.0625°$. If this is not obtained at 120 knots, then the same test will be performed at 150 knots since that is the highest velocity allowed by the wind tunnel. Testing at 50 knots will also be conducted since that is the lowest velocity the static test for the F-16 AOAT is performed. If this is not achievable, then a hot-wire can be used and the same experiment repeated to see if the hot-wire will produce better results.

4.3   Testing Results

Data was collected from each probe for at least 100 rolling average samples, which took approximately 1.5 minutes to collect at each set of data. The results from this test varied between each probe at 120 and 150 knots using the original probe support fixture, which does not allow any alignment of the axis of the probe. The typical measurements obtained from these probes is shown in probe SN71327010, shown in Fig. 4.1 and Fig. 4.2 for the results at 120 knots and Fig. 4.3 and Fig. 4.6 for the results at 150 knots. The results from all of the probes are shown in the appendix in Fig. A.1 - Fig. A.24.

The data in Fig. 4.1 - Fig. 4.4 show that there is a high amount of noise associated with probe SN71327010 at 120 and 150 knots. These are typical of the results found between all of the other probes used. There also appears to be a slight general upwards trend to the data over time, causing the uncertainty of the data to also increase. This drift can easily
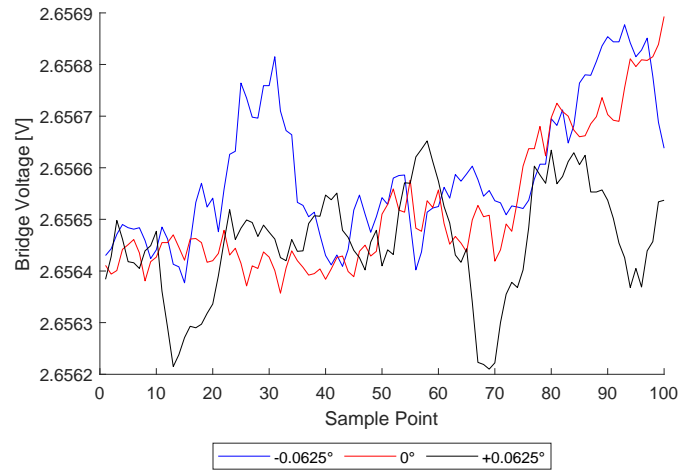
Fig. 4.1: Bridge voltages at calibrator from sensor 1 on SN71327010 at $-0.0625°$, $0°$, and $+0.0625°$ at 120 knots
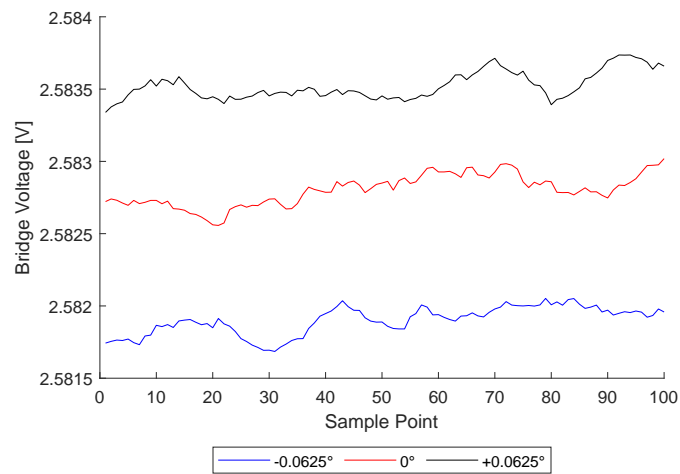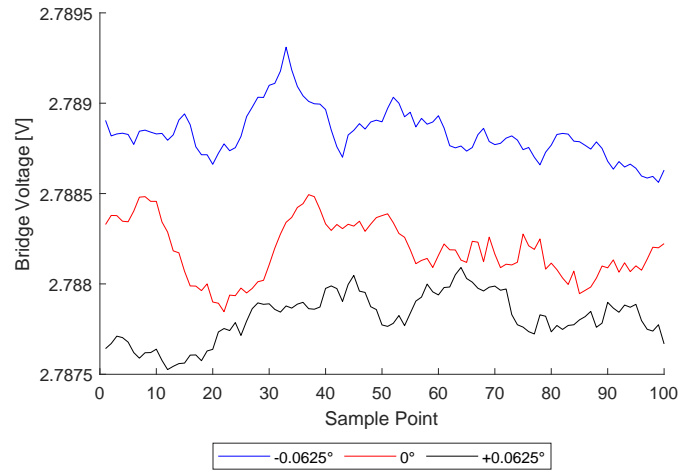

Fig. 4.2: Bridge voltages at calibrator from sensor 2 on SN71327010 at $-0.0625°$, $0°$, and $+0.0625°$ at 120 knots

Fig. 4.3: Bridge voltages at calibrator from sensor 1 on SN71327010 at −0.0625°, 0°, and +0.0625°at 150 knots

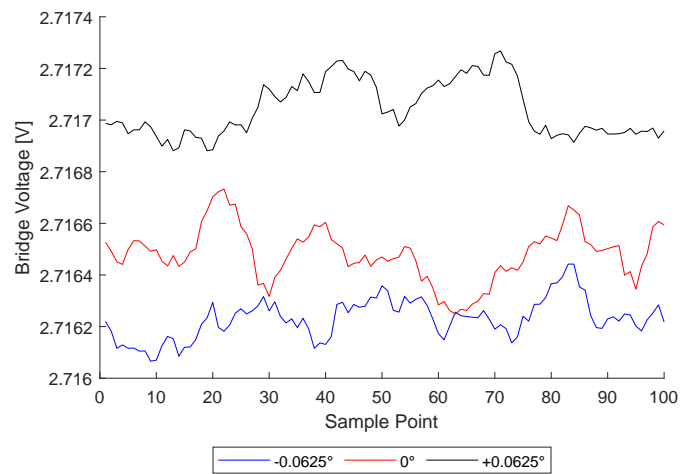Fig. 4.4: Bridge voltages at calibrator from sensor 2 on SN71327010 at −0.0625°, 0°, and +0.0625° at 150 knots

be eliminated by calculating the differential between the E_1 and E_2 voltages, however, this reduces the data from two variables to one and does not allow Jorgensen's two-dimensional equations to be used. The standard deviation and mean of the collected data were calculated and the results plotted to show if the noise from $\pm0.0625°$ overlapped with the noise at $0°$. The rolling average data, the mean of the data, as well as the noise represented as plus or minus three standard deviations, or $\pm3\sigma$ from the mean was plotted to compare the results. Since there are two voltages referred to with each angle and velocity reading, looking at this data by creating a voltage differential between the two voltages to observe if three standard deviations of the differential data interfere with the angle data at $-0.0625°$, $0°$, and $0.0625°$ is a simpler way to see if the readings interfere with each other. This data is shown in Fig. A.25 and Fig. A.36 for SN71327010. The results obtained from all of the probes is shown in Fig. A.25 - Fig. A.36.
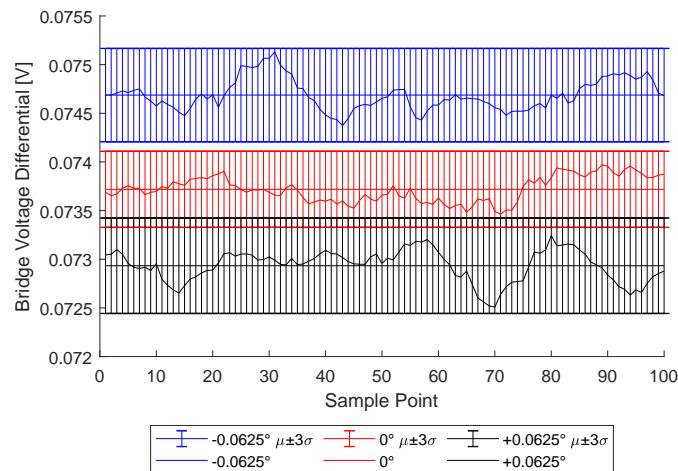
Fig. 4.5: Differential bridge voltages at calibrator (sensor 2 bridge voltage minus sensor 1 bridge voltage) on SN71327010 at $-0.0625°$, $0°$, and $+0.0625°$ at 120 knots with $\pm3\sigma$ Standard Deviations

During this time, it was also observed that the noise changed significantly depending on the TSI probe support on which the probe was installed. One example of this is shown in Fig. 4.7. This shows the amount of noise from probe SN7132010 when it was installed on
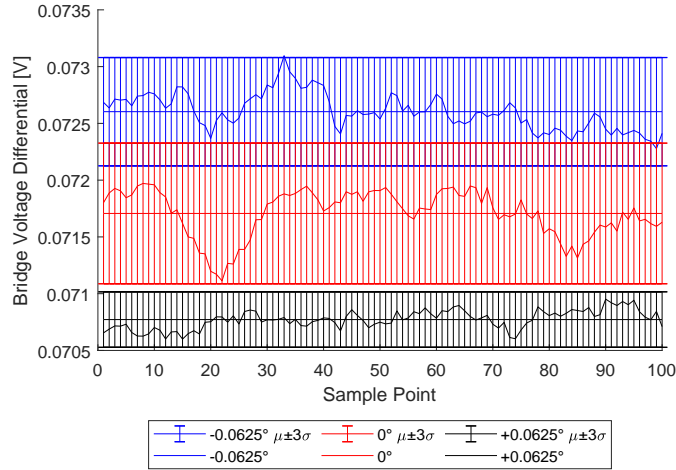
Fig. 4.6: Differential bridge voltages at calibrator (sensor 2 bridge voltage minus sensor 1 bridge voltage) on SN71327010 at $-0.0625°$, $0°$, and $+0.0625°$ at 150 knots with $\pm 3\sigma$ Standard Deviations

one probe support, which was large. The probe was then installed on a different TSI probe support, and the characterization results are shown in Fig. 4.8. Variations in the amount of noise may be due to a damaged TSI probe support during handling. Consequently, it was noted when a probe responded well to a specific TSI probe support to further reduce noise from measurements with that probe.

In order to compare using a one-dimensional look-up table made by taking a differential of the two voltage readings from the sensors with the classic two-dimensional look-up table, one probe was selected and measurements at $\pm 2.5°$, $\pm 2°$, $\pm 1.5°$, $\pm 1.0°$, $\pm 0.5°$, $\pm .1°$, $\pm 0.0625°$, $\pm 0.03°$, and $0°$ were collected. The probe was then validated at the calibrator by using a one-dimensional look-up table with a voltage differential between the two sensors and using the spline MatLab function. Then, a classic two-dimensional look-up table method was conducted with the griddata MatLab function. The probe was also placed in the wind tunnel and readings from the two-dimensional and one-dimensional look-up table were obtained. Table 4.1 shows the data points that were captured to compare these readings.

Table 4.1 shows that using a two-dimensional look-up table is slightly more accurate
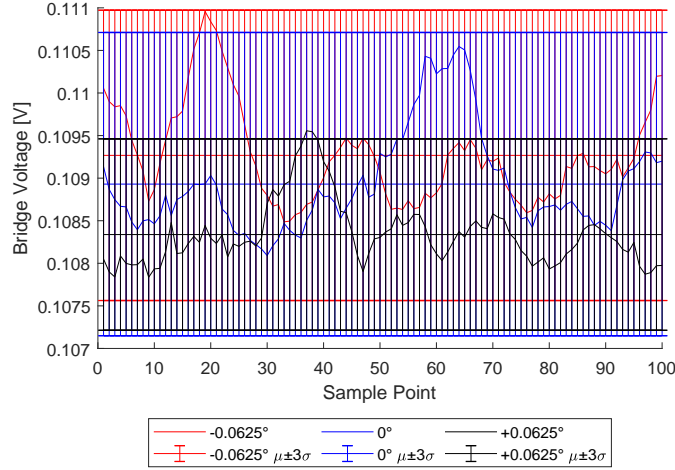
Fig. 4.7: SN71327010 on the first TSI 1155 probe support with three standard deviations of noise at 120 knots and $-0.0625°$,$0°$, and $+0.0625°$.

Validation at 0°at Calibrator		Front of Wind Tunnel		Back of Wind Tunnel	
One-Dimensional	Two-Dimensional	One-Dimensional	Two-Dimensional	One-Dimensional	Two-Dimensional
$-0.0049°$	$-0.0001°$	$-2.0865°$	$-2.0854°$	$-1.8277°$	$-1.8424°$

Table 4.1: Comparison of look-up table using a voltage differential and a two dimensional look-up table method with probe SN71327011.

than a one-dimensional lookup table, since the two-dimensional look-up table is much closer to $0°$ than the one-dimensional look-up table is. However, each of the readings from a one-dimensional look-up table are still well within $0.0625°$ to the readings from the two-dimensional look-up table. This fact justifies using a one-dimensional look-up table for the remainder of the experiments. This was chosen due to the time-consuming nature of obtaining the measurements needed for a two-dimensional look-up table. One that was developed during testing with 3 velocities and 17 angles took over 4 hours to complete due to collecting 1.5 minutes of data for every data point. Even with this differential performed, some probes still produce noise that shows interference with readings at 0 and $\pm0.0625°$.

After characterization, calibration, and validation utilizing Jorgensen's equation were performed on each probe before being placed in the wind tunnel. During measurement, the wind tunnel velocity indicator was set to 50,70, 90, 110, 120, and 130 knots. The difference
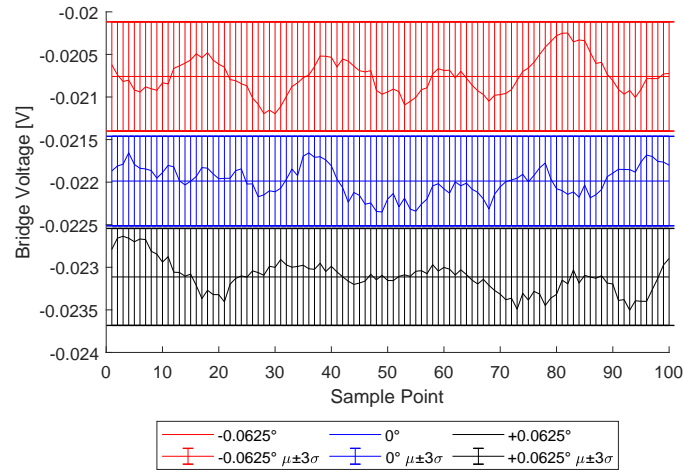
Fig. 4.8: SN71327010 on the second TSI 1155 probe support with three standard deviations of noise at 120 knots and $-0.0625°, 0°$, and $+0.0625°$.

between the velocity indicator and the probe were recorded. The velocity of the wind tunnel was then set to 120 knots and the angle reading recorded. This was then repeated on the opposite side of the wind tunnel test section. The first probe used to perform this test was the hot-wire probe SN71201084, and it was concluded in Fig. A.3, Fig. A.4, Fig. A.15, Fig. A.16, Fig. A.26, and Fig. A.32 that the noise at $±0.0625°$ and $0°$ for this probe do not interfere with each other. Since the alignment plate on the front side of the wind tunnel has been accepted as being calibrated by engineering authority, it was not adjusted, but a measurement was recorded from this side. The alignment plate on the back side of the wind tunnel is currently not used for calibration, and has not been accepted as being calibrated, so the plate on the back side can be rotated for experimental purposes. Table (4.4) shows the results from each probe for the validation as well as velocity and angle measurement phases.

These results show that none of the angle measurements from the probes at the wind tunnel agree with each other. They also show that the probes measured up to almost $4°$ different from each other. However, given the tolerance of $±5$ knots for each velocity measurement, each probe agrees with each other and to this tolerance. It is expected that

Probe Serial Number	50 knots	70 knots	90 knots	110 knots	120 knots	130 knots
SN71201084	52.238	71.785	90.914	110.555	120.525	130.152
SN71201083	54.382	73.057	93.380	111.630	121.524	130.747
SN71201086	52.546	71.309	90.317	109.343	118.658	128.336
SN71327010	51.441	71.441	91.753	111.608	120.347	129.943
SN71327011	52.360	72.594	91.880	111.176	120.071	130.632
SN71430019	54.605	74.140	94.417	113.986	124.811	133.769

Table 4.2: Wind tunnel airspeed results from each X-probe compared with the wind tunnel velocity indicator readings

Probe Serial Number	50 knots	70 knots	90 knots	110 knots	120 knots	130 knots
SN71201084	53.323	71.854	91.010	109.857	120.038	129.789
SN71201083	50.280	71.274	89.708	109.244	118.598	127.715
SN71201086	52.176	71.420	90.326	108.871	118.729	128.162
SN71327010	51.865	71.275	91.204	110.371	119.897	129.268
SN71327011	52.044	71.793	91.549	110.004	120.173	129.607
SN71430019	52.786	72.360	94.163	114.040	124.156	133.371

Table 4.3: Velocity measurements for each probe on the front side of the wind tunnel after using the calibration method based on Jorgensen's equation. Measurements are compared to the readout from the wind tunnel velocity indicator.

Probe Serial Number	Validation Average Angle	Front Side of Wind Tunnel Average Angle at 120 knots	Back Side of Wind Tunnel Average Angle at 120 knots
SN71201084	$-0.0009°$	$-0.2981°$	$-0.0039°$
SN71201083	$0.0201°$	$-3.2642°$	$-3.0243°$
SN71201086	$-0.0034°$	$-0.2088°$	$0.0461°$
SN71327010	$-0.0005°$	$-1.2728°$	$-1.0987°$
SN71327011	$-0.0316°$	$-2.8306°$	$-2.6364°$
SN71430019	$0.4706°$ (Failed)	$-3.9329°$	$-3.7095°$

Table 4.4: Angle measurements from each probe after calibrating the back side of the wind tunnel to be zero according to SN71201084 after using the calibration method based on Jorgensen's equation.

when each probe is placed at the wind tunnel, the angle and velocity measurements will agree with each probe, since all but one probe passed the validation for angle measurements. In order to determine why each probe does not agree with each other's angle measurement, possible error sources will be investigated and reduced as much as possible.

Velocity measurements from the X-probes were also verified by a Kiel probe to obtain true airspeed in the wind tunnel test section. This was achieved by using Eq. (4.1) and (4.2), where V is the true airspeed, K is the pitot flow coefficient (which is 1.0 for the Kiel probe used), P_{abs} is the static pressure, T is the temperature of the flow in Celsius, R is the gas constant for air, and ΔP is the differential pressure between the static pressure found from a static pitot tube and the Kiel probe. The equations are from the instructions given by Flowkenetics [6] who manufactured the Kiel probe used in this experiment. The velocity at each required set point for the wind tunnel was measured and calculated. These results can be found in Table (4.5).

$$V = K\sqrt{\frac{2\Delta P}{density}} \tag{4.1}$$

$$density = \frac{P_{abs} + (1 + K^2)\Delta P}{R(T + 273.15)} \tag{4.2}$$

Wind Tunnel Indicator Velocity	50 knots	70 knots	90 knots	110 knots	120 knots	130 knots
Kiel Probe Velocity	50.152	69.518	89.001	108.332	119.460	129.053

Table 4.5: Results from comparing the Kiel probe velocity to the wind tunnel velocity indicator

Since the velocity measurements for each X-probe passed the ± 5 knot requirement, and all readings from the Kiel probe agree within 5 knots of the readings from the wind tunnel velocity indicator, the velocity calibration meets the velocity requirements, and the remainder of the testing results will focus on the angle alignment and not the velocity

calibration.

4.3.1   Reduction of Velocity to 50 knots

The first source of error that will be investigated is the random noise from each probe. One possible source of this noise could be vibration from from the air hitting the probe during calibration. In order to find this error, the noise for each probe at 50 knots and at $\pm0.0625°$ and $0°$ was evaluated. The results from the tests at 50 knots on SN71327010 can are shown in Fig. 4.9 and Fig. 4.10 the results from characterization of all of the probes at 50 knots are found in the appendix in Fig. A.37 - Fig. A.44. One thing to note with this test is that before all the data could be obtained from all of the probes, some of them were damaged or broken. This means that readings could not be obtained from these probes. Therefore, these figures contain only the information gathered from the available probes.
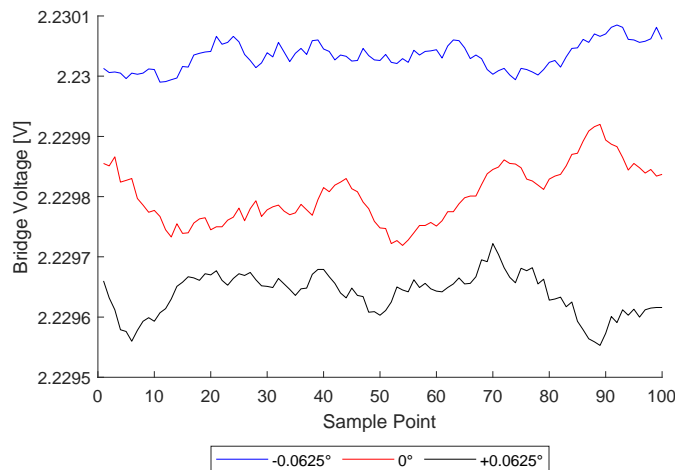
Fig. 4.9: Bridge voltages at calibrator from sensor 1 on SN71327010 at $-0.0625°$, $0°$, and $+0.0625°$ at 50 knots

The differential was then calculated between the bridge voltage from sensor 1 and sensor 2. The calculated voltage differential between the two sensors from testing SN71327010 at 50 knots are shown in Fig. 4.11. The results of all of the probes for this test is shown in
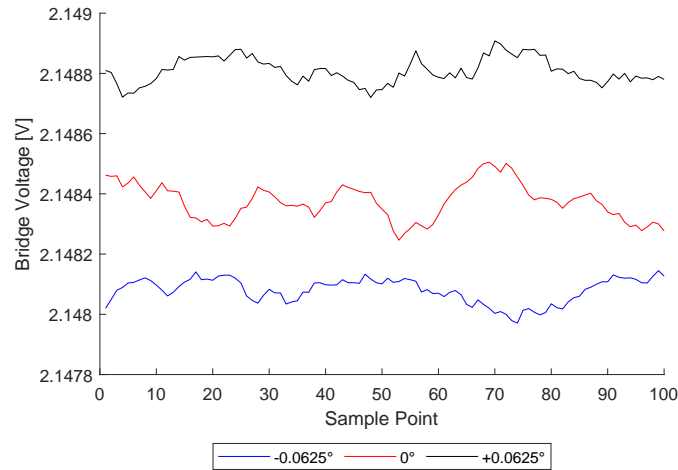
Fig. 4.10: Bridge voltages at calibrator from sensor 2 on SN71327010 at $-0.0625°$, $0°$, and $+0.0625°$ at 50 knots

the appendix in Fig. A.45 - Fig. A.48.
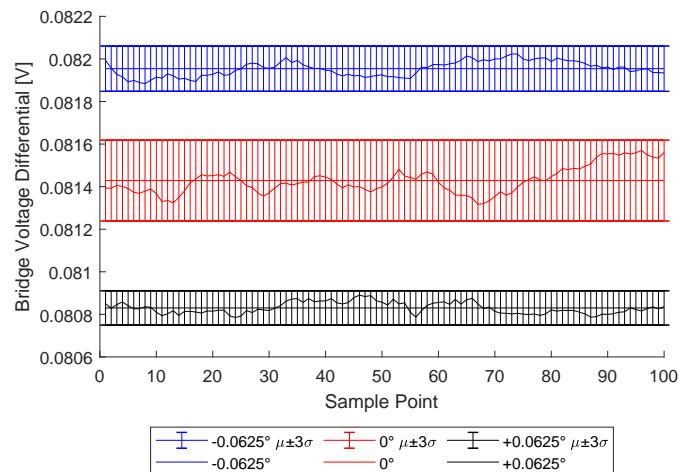
Fig. 4.11: Differential bridge voltages at calibrator (sensor 2 bridge voltage minus sensor 1 bridge voltage) on SN71327010 at $-0.0625°$, $0°$, and $+0.0625°$ at 50 knots with $\pm3\sigma$ Standard Deviations

Results at 50 knots show that the noise at $\pm0.0625°$ and $0°$ is significantly reduced from the noise at 120 and 150 knots. Since the F-16 AOAT is tested for static friction at

50 knots as well as 120 knots, this speed was used for further testing to reduce noise and investigate possible solutions to obtaining consistency between multiple probes, SN71327010 and SN71430019. Calibration using the method based off of Jorgensen's equation was conducted, but all angle measurements were obtained at 50 knots instead of 120 knots. Both probes passed the validation mode, by measuring less than $\pm 0.0625°$ at 50 knots after calibration. As shown in Table (4.6), the alignment plate on the backside of the wind tunnel was then aligned to $-0.0034°$ with SN71327010, and measured $-1.8010°$ on the front side of the wind tunnel. SN71430019 measured $-2.0746°$ on the front side of the wind tunnel, and $-0.8366°$ on the back side of the wind tunnel, showing that reducing the noise by reducing the velocity to 50 knots did not allow wind tunnel measurements between multiple probes to agree.

Probe SN	Front Side Wind Tunnel Angle Reading	Back Side Wind Tunnel Angle Reading
SN71327010	$-1.8010°$	$-0.0034°$ (zeroed)
SN71430019	$-2.0746°$	$-0.8366°$

Table 4.6: Wind tunnel readings after Jorgensen's equation calibration at 50 knots on original probe support fixture.

To eliminate the possibility that these variations in measurements from each probe are occurring because the probe is not axially aligned with the rotation stage, a new probe support fixture was made. This new support was manufactured with four set screws, each $90°$ apart from each other and located on the tip of the probe support fixture so that the screws could be adjusted to align the probe with the rotation stage axis. By using a dial indicator, the probe axis and the rotation stage axis were aligned to within ± 0.0005 inches. After this alignment was performed, probes SN71327011 and SN71327010 were calibrated with the Jorgensen's equation method and used to take angle measurements of the alignment plates on both sides of the wind tunnel.

Both SN71327011 and SN71327010 passed validation after calibration with angle validation numbers being $-0.0089°$ for SN71327011 and $-0.0046°$ for SN71327010. However,

as shown in Table (4.7), when measured at the wind tunnel at 50 knots, the angle measurements were found to be $-1.9487°$ on the front side of the wind tunnel for SN71327011, compared to $-2.1830°$ for SN71327010. The back side of the wind tunnel was calibrated to $-0.0041°$ using SN71327011, however, SN71327010 gave a reading of $1.0325°$ on this same side. These results show that simply aligning the rotation axis of the probe to the rotation stage does not allow the measurements from multiple probes to agree.

Probe SN	Front Side Wind Tunnel Angle Reading	Back Side Wind Tunnel Angle Reading
SN71327010	$-2.1830°$	$1.0325°$
SN71327011	$-1.9487°$	$-0.0041°$ (zeroed)

Table 4.7: Wind tunnel readings after Jorgensen's equation calibration at 50 knots on modified probe support.

4.3.2 Elimination of Jorgensen's Equation Assumptions

As previously mentioned in Chapter (1), the calibration method based on Jorgensen's equation has multiple assumptions. The first assumption is that the sensors are perpendicular to each other, which is used to develop equations for finding the angle of the flow over the sensor. The second assumption is that at $0°$ angle of attack, the direction of the air flow bisects the angle between the two sensors. It is virtually impossible for two wires to be exactly perpendicular to each other, as well as the flow to exactly bisect the two sensors, causing a measurement error when this assumption is made.

In order to eliminate the assumption of the two sensors being perpendicular to each other, a look-up table method was formed. This would allow the error due to these assumptions to be quantified. In order to produce a successful look-up table, the noise from a probe at a set angle point must not interfere with other points in the look-up table. As discussed earlier, the bridge voltages from each sensor have a tendency to drift upwards as time passes. This can be eliminated, as previously explained, by subtracting the voltage measured between each sensor to form a voltage differential. However, this will eliminate

the two variables for voltages needed to form a look-up table such as the one formed by Lueptow et al. [9].

Since the calibration requirements of the wind tunnel do not require a variety of angles to be known at multiple velocities, this differential can be used to form a one-dimensional look-up table for a specific velocity, which can be determined by the calibrated wind tunnel velocity indicator. A look-up table can then be formed by measuring the X-probe voltages at the calibrator for only one velocity. The rotation stage is then set to multiple angles to form a look-up table for angles at one velocity. The MatLab function spline, a cubic spline interpolation function, is used to interpolate the angle measurements at the wind tunnel with the one-dimensional look-up table to determine the angle from the bridge voltage readings.

In order to further reduce the noise from each angle measurement at the calibrator, the angle measurements were performed at 50 knots. This is due to results from the noise tests which show that if the calibration is performed at 50 knots there will be less noise than if taken at 120 or 150 knots. Again, probes SN71327010 and SN71327011 were used for this look-up table. The bridge voltages were recorded for each sensor at 50 knots and the rotation stage set to $\pm 2.5°$, $\pm 2.0°$, $\pm 1.5°$, $\pm 1.0°$, $\pm 0.5°$, $\pm 0.1°$, $\pm 0.0625°$, $\pm 0.03°$, and $0°$. Over 100 data points were collected by using the 10 point rolling average for each angle setting and the average of the bridge voltages at each angle were recorded. The differential between the bridge voltages was calculated and recorded as the look-up table set point for each angle.

After the look-up table was formed, the probes were taken to the wind tunnel and the wind tunnel velocity indicator set to 50 knots. Bridge voltages from each sensor were read and recorded, and also subtracted from each other in order to use the differential voltage look-up table. First, probe SN71327011 was used to measure the angle from the front side of the wind tunnel with a reading of $-2.1068°$, where SN71327010 measured $-1.0762°$. On the back side of the wind tunnel, SN71327011 was used to calibrate the alignment plate until it read $0.0170°$. Probe SN71327010 then measured $1.1395°$ on the back side of the

wind tunnel. These results are shown in Table (4.8). Comparing the measurements from these two probes reveal that a look-up table does not provide consistent measurements of 0° at the Hill AFB wind tunnel between multiple probes.

Probe SN	Front Side Wind Tunnel Angle Reading	Back Side Wind Tunnel Angle Reading
SN71327011	$-2.1068°$	$0.0170°$ (zeroed)
SN71327010	$-1.0762°$	$1.1395°$

Table 4.8: Wind tunnel readings after look-up table calibration at 50 knots.

It was expected that using a look-up table and the modified probe support fixture to align the probe with the axis of the rotation stage would result in measurements that were consistent between probes. As stated by Fingerson and Freymuth [3] in the literary review, a thermal anemometer calibration is only as reliable as the conditions during calibration and measurement coinciding with each other. The fact that these measurements are so different from each other hinted that there could be some conditions that vary between the wind tunnel and the calibrator. An investigation was conducted with the test section of the wind tunnel to see if there was some nonconformity. It was discovered that the distance between the sidewalls of the test section closest to the inlet of the wind tunnel measured 12 inches while the distance between the sidewalls of the test section closest to the outlet measured 12.125 inches . A second wind tunnel at Hill AFB that is the same model number as the current wind tunnel, but is not in service, was also measured and found to have the same measurements for the test section. After further research, it was discovered that it is normal for test sections of wind tunnels to have a slight divergence to achieve a constant static pressure [23].

Wind tunnels commonly have walls that diverge to compensate for a thickening boundary layer and maintain a constant value of static pressure through the test section [23]. However, over the last 10 years that this wind tunnel has been in operation, it was unknown that the walls of the wind tunnel test section were not square. This difference in width from one end of the test section to the other will cause the probe to be oriented so

that the free air stream in the wind tunnel is not perpendicular to the probe. Since the test section is 24 inches long, if it is assumed that each side of the test section of the wind tunnel has flared half of 0.125 inches on each side (or 1/16 inch flare on each side), the angle of the air stream to the probe when placed in the wind tunnel can be calculated. The angle can be calculated by $sin^{-1}\left(\frac{0.125\,inches}{24\,inches}\right)$, which equals 0.149°. This means that in order to compensate for this angle during calibration, the probe must be offset by orienting it 0.149° towards the air stream in order to be perpendicular to the flow in the wind tunnel.

To deflect the probe by this amount, a dial indicator was placed 1.35 inches away from the plug of the hot-film probe. The set screws on the modified probe support fixture were then adjusted so that the probe pointed 0.0035 inches towards the air stream. This deflection should have compensated for the change in width of the test section and made the probe perpendicular to the flow in the wind tunnel during measurement.

Since SN71327010 and SN71201086 broke and were no longer usable, two hot-film probes, SN71430019 and SN71327011 were each calibrated with the new probe support fixtures. These two probes were then adjusted to compensate for the wind tunnel walls flaring outwards. This was performed by first aligning each of their axes to the rotation stage by using a dial indicator to ensure there was less than 0.0005 inches of run-out as each probe was rotated 360°. Next, each probe was characterized to ensure the noise from each probe was not so large that the measurement at −0.0625° would interfere with the readings at 0° and also to ensure that readings at 0.0625° did not interfere with the readings at 0°.

Both probes were then calibrated using a look-up table method, and validated to be within ±0.0625 of the angle reading from the rotation stage. Next, each probe was deflected by 0.0035" towards the air stream of the calibrator by using the alignment set screws of the redesigned probe support fixture and then validated again. Table (4.9) shows the validation results before and after this deflection at the calibrator.

The results shown in Table (4.9) show that by deflecting the probe, SN71430019 was virtually unaffected, and still passed validation by reading 0° ± 0.0625°, however, SN71327011 failed validation after being deflected. This shows that each probe is affected differently

Probe SN	Angle Reading Before Deflection at 0°	Angle Reading After 0.0035" Deflection at 0°
SN71430019	$-0.0037°$	$-0.0015°$
SN71327011	$-0.0049°$	$-0.0842°$

Table 4.9: SN71430019 and SN71327011 angle validation results at the calibrator before and after deflecting the probe by 0.149° towards the air stream of the calibrator

when its orientation is adjusted and a binormal velocity component affects the probe.

Next, each probe is placed in the wind tunnel. First, readings were taken from SN71430019 on the front and back side of the wind tunnel. The alignment plate on the back side of the wind tunnel was then aligned to within $0 \pm 0.0625°$ with probe SN71430019. Probe SN71327011 was then installed on the front and back side of the wind tunnel and angle readings were taken and recorded. Table (4.10) shows the reading results from each probe.

Probe SN	Front Side Wind Tunnel Angle Reading	Back Side Wind Tunnel Angle Reading
SN71430019	$-0.2132°$	$-0.0042°$
SN71327011	$-2.0865°$	$-1.8277°$

Table 4.10: SN71430019 and SN71327011 measurements at wind tunnel after deflecting the probe by 0.149° towards the air stream

The results in Table (4.10) show that an attempt at correcting for the deflection of the X-probe due to the wind tunnel walls not being parallel did not solve the measurement inconsistencies between each probe.

There are many reasons why this correction did not fix the consistency problem between probes, such as the deflection of the probe bending the plugs and changing the voltage readings, or a cross-flow in the wind tunnel cause by leaks in the wind tunnel [23]. Leaks in the test section were tested with a bottle of soapy water. It was found that there was a leak in the bottom corner of the test section, which could cause disturbance to the flow during measurement. In order to fully diagnose and fix any leaks, the wind tunnel must be

evaluated with smoke or other visualization materials that will allow the effects of the leaks to be seen in order to be fixed. Attempts were not made to fix these leaks since a higher engineering authority would need to approve any changes to the configuration of the wind tunnel.

CHAPTER 5

Conclusions and Recommendations

The testing performed on the hot-wires and hot-films resulted in several recommendations to perform highly accurate measurements for angle alignment. These recommendations are expounded upon in this section.

1. The conditions at this wind tunnel do not match the conditions simulated with the calibrator.

2. A full evaluation of the wind tunnel must be conducted in order to fully understand the differences between the wind tunnel and calibrator.

3. It was inconclusive if the method based on Jorgensen's equation or a look-up table could achieve the calibration requirements at the wind tunnel.

4. The characterization of each probe by taking readings at multiple velocities and angles is an important step when using a thermal anemometer probe as a calibration device.

5. Although the literature review states that using a hot-wire will generally reduce noise, this was not confirmed by the experiments conducted since only two hot-wires were available for experimentation.

6. After testing hot-wire and hot-film X-probes, it is also apparent how fragile these probes are. This alone makes a thermal anemometer an unsuitable candidate to perform frequent alignments and velocity calibrations.

7. Further adjustment may need to be made on the specification provided by engineering authority of the alignment plate being within $\pm 0.0625°$ of the free stream velocity.

Conditions Must Match   No two X-probes could agree with each other's measurements at the wind tunnel, even though each probe could pass validation to within $\pm 0.0625°$ at

the calibrator with either a look-up table method, or using Jorgensen's equation. This shows that each probe can measure both angle and velocity accurately when compared to the velocity obtained from the differential pressure transducer and the angle from the rotation stage. However, once conditions change by placing the X-probe in the wind tunnel, the measurements from the X-probe are no longer reliable, which can be concluded from the inconsistent measurements from each probe (see Tables (4.4), (4.8), and (4.10)). This coincides with the literature survey, which states that no matter which method is used for calibration, errors will result from any differences between the calibrator and the wind tunnel. Possible reason to these inconsistencies are due to leaks into the wind tunnel test section from the mounting plates not being fully sealed, which would cause a binormal velocity [23].

Tests to determine the conditions which vary between the calibrator and the wind tunnel at Hill AFB were inconclusive. It was found that a possible inconsistencies is from the walls of the wind tunnel test section diverging by $0.149°$ on each side. After research, it was found that this is normal to have a diverging test section in a wind tunnel to account for the boundary layer [23]. Compensation for this divergence was attempted with two hot-film probes place on modified probe supports. Even with this compensation, it was not possible to have two probes agree with each other's measurement at the wind tunnel. Experiments were performed at the calibrator by adding a binormal velocity by deflection through the probe support fixture show that each probe is affected differently when two-dimensional velocity is assumed, but three-dimensional velocity is actually occurring. This means that it is possible that measurements from each probe being different could be caused by a unaccounted for binormal velocity. It can be noted that deflecting the hot-film probe in this manner may alter the calibration scheme. The voltage readings could change by simply bending the plug wires, and may not be a valid way to compensate for the diverging walls in the test section.

Tests were performed to discover if there were any leaks in the wind tunnel. It was found during these tests that there were indeed leaks from the plates mounted on the wind

tunnel test section by using a water and soap mixture. Any of these leaks could produce turbulence or a side angle of air stream that could cause errors in measurements. To fully investigate these leaks, it is recommended that smoke or another visualization tool is used to detect and fix these leaks. An attempt to seal these leaks was not performed since it required higher approval to adjust the design of the certified test section of the wind tunnel.

Full Evaluation of Wind Tunnel

A full evaluation of the wind tunnel could include measuring the wind tunnel with accurate three-dimensional scanning devices, as well as ways to visualize the flow in the wind tunnel test section. Another option to fully characterize the flow and align devices on a wind tunnel is to use a hot-film or hot-film probe that has at least three sensors. This would allow the flow to be measured in all three directions, allowing the entire velocity vector to be found. This process would require a new calibration stand to be used at Hill AFB, which would need to be designed to calibrate along all three axes, and require more funding than is available for this project.

Jorgensen's Equation Versus Look-up Table

Although neither Jorgensen's method or the look-up table successfully calibrated the alignment plate on the wind tunnel, both methods consistently passed validation at the calibrator when conditions were the same during calibration and validation. However, the inconsistencies between probe measurements at the wind tunnel made it impossible to fully compare the calibration of the probes using Jorgensen's equation or a look-up table.

Characterization

Each system and probe is unique, so by recording measurements for a long period of time, trends can be observed, allowing steps to be made to eliminate any noise or other measurement problems. Then, variables can be eliminated one by one until the problem is found that limits the accuracy of the system, or it is realized that the anemometer probe will not achieve the needed requirements.

Hot-wire Versus Hot-film

It was found that the noise in the readings from one hot-wire had significantly less noise than any of the hot-films. However, the other hot-wire probe had significantly more noise than the first, and was comparable to noise from the hot-film probes. From the characterization of the probes, it appears that each probe had their own unique value of noise associated with it. Since the same equipment was used to calibrate each probe, it appears that this variation in noise is produced by the X-probe itself, or the probe support, and not the calibration equipment. These differences are assumed to be due to the way each probe was manufactured, such as the angle the sensors are oriented to each other, or the process of attaching these wires or films to the prongs which support them.

Fragility of X-probes

The fragility of the X-probes alone makes a thermal anemometer not suitable candidate to perform frequent alignments and velocity calibrations. During this investigation on the Hill AFB wind tunnel alone, multiple probes were damaged or broken, which may be expensive to repair or replace. For other wind tunnels, when a thermal anemometer is being used, great care must be taken to ensure that the probe is not broken. It is also recommended that a pitot tube, or another pressure differential measuring probe are investigated first before a thermal anemometer is used to perform frequent wind tunnel calibrations.

Examination of Requirements

The requirement given for the alignment of the wind tunnel plate appears to be restrictive and not realistic compared with other wind tunnel measurement devices, which commonly have an accuracy between $\pm 0.5°$ to $\pm 1.0°$. If the angle alignment tolerance were to be widened, the options of using other equipment that could provide faster and more reliable calibration could be used. As discussed in section 3.1, engineering authority has the ability to determine the requirements of the wind tunnel, such as was performed when the decision was made that the plate itself did not provide a measurement, but was aligned with

an instrument that had an accuracy of $\pm 0.0625°$. There may be a way to find acceptable tolerances for new test equipment that are not too stringent. This can be performed if the actual requirements of the aircraft are known and examined to determine the requirements of the instrument being tested on the wind tunnel. Although this may be information that is difficult to, it will enable a more realistic and accurate requirement to be given for the wind tunnel.

REFERENCES

[1] Jorgensen, F. E., "Directional sensitivity of wire and fiber-film probes. An experimental study." *DISA Information No. 11*, May 1971, pp. 31–37.

[2] Lekakis, I., "Calibration and signal interpretation for single and multiple hot-wire/hot-film probes," *Meas. Sci. Techol.*, Vol. 7, 1996, pp. 1313–1333.

[3] Fingerson, L. M. and Freymuth, P., *Thermal anemometers*, chap. 3, Hemisphere Publishing Corp., 1983, p. 99.

[4] Aeroprobe, *Conventional probes*, 2017.

[5] Kiel, G., "Total-head meter with small sensititivity to yaw." TM 775, NACA, 1935.

[6] FlowKinetics, *Kiel probes*, FlowKinetics LLC, 4700 Shoal Creek Dr, College Station, TX 77845, 2018.

[7] King, L. V., "On the convection of heat from small cylinders in a stream of fluid: determination of the convection constants of samll platinum wires with application to hot-wire anemometry," *Phil. Trans. R. Soc.*, Vol. 214, 1914, pp. 373–432.

[8] Bradshaw, P., *An introduction to turbulence and its measurement.*, Oxford: Pergamon Press, 1971.

[9] Lueptow, R. M., Breuer, K. S., and Haritonidis, J. H., "Computer-aided calibration of X-probes using a look-up table," *Experiments in Fluids*, Vol. 6, 1988, pp. 115–118.

[10] Hinze, J. O., *Turbulence*, McGraw-Hill, 2nd ed., 1975.

[11] Gilmore, D. C., *The probe interference effect of hot-wire anemometers*, Montreal, Mechanical Engineering Research Laboratories, McGill University, 1967.

[12] Ovink, R., Lamers, A. P. G. G., van Steenhoven, A. A., and Hoeijmakers, H. W. M., "A method of correction for the binormal velocity fluctuation using the look-up inversion method for hot-wire anemometry," *Measurement Science and Technology*, 2001, pp. 1208–1213.

[13] Burattini, P. and Antonia, R., "The effect of different X-wire calibration schemes on some turbulence statistics," *Experiments in Fluids*, Vol. 38, 2005, pp. 80–89.

[14] Willmarth, W. W. and Bogar, T. J., "Survey and new measurements of turbulent structure near the wall." *Physics of Fluids*, Vol. 20, No. 10, 1977, pp. S9–S21.

[15] Johnson, F. D. and Eckelmann, H., "A variable angle method of calibration for X-probes applied to wall-bounded turbulent shear flow." *Experiments in Fluids*, Vol. 2, 1984, pp. 121.

[16] Zilberman, M., *On the interaction of transitional spots and generation of a synthetic turbulent boundary layer*, Ph.D. thesis, Tel-Aviv University, 1981.

[17] van Dijk, A. and Nieuwstadt, F. T. M., "The calibration of (multi-) hot-wire probes. 1. Temperature calibration." *Experiments in Fluids*, Vol. 36, 2004, pp. 540–549.

[18] TSI, *Innovation in thermal anemometry*, 1998.

[19] Benjamin, S. F. and Roberts, C. A., "Measuring flow velocity at elevated temperature with a hot wire anemometer calibrated in cold flow," *International Journal of Heat and Mass Transfer*, Vol. 45, 2002, pp. 703–706.

[20] Ardekani, M. A. and Farhani, F., "Experimental study on response of hot wire and cylindrical hot film anemometers operating under varying fluid temperatures," *Flow Measurement and Instrumentation*, 2009.

[21] Bruun, H. H., Nabhani, N., Fardad, A. A., and Al-Kayiem, H. H., "Velocity component measurements by X hot-wire anemometry," *Measurement Science and Technology*, Vol. 1, 1990, pp. 1314–1321.

[22] Cengel, Y. A. and Cimbala, J. M., *Fluid mechanics fundamentals and applications*, McGraw-Hill, 2nd ed., 2009.

[23] Barlow, J. B., William H. Rae, J., and Pope, A., *Low-speed wind tunnel testing*, Wiley, 1999.

APPENDICES

APPENDIX A

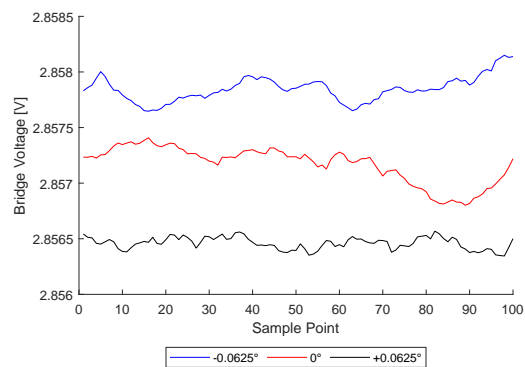Figures of Results

A.1 Rolling Average Voltages at 120 Knots
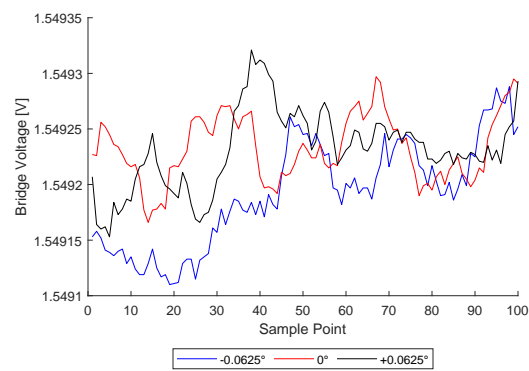
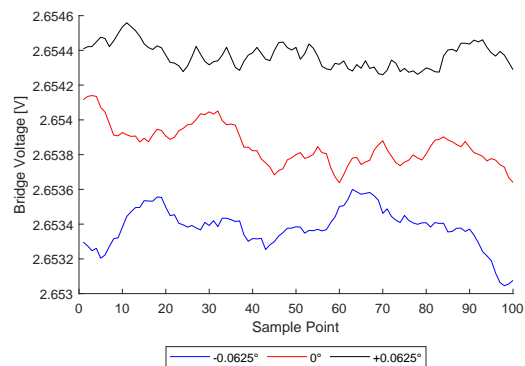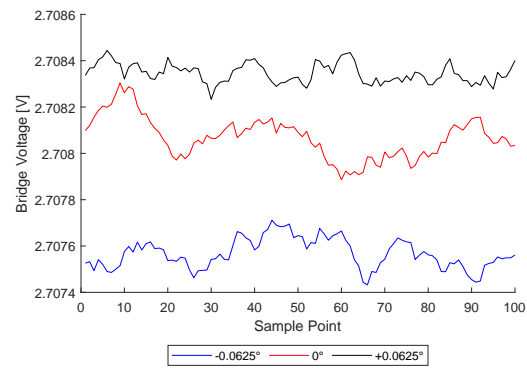Fig. A.1: Bridge voltages at calibrator from sensor 1 on SN71201083 at $-0.0625°$, $0°$, and $+0.0625°$ at 120 knots
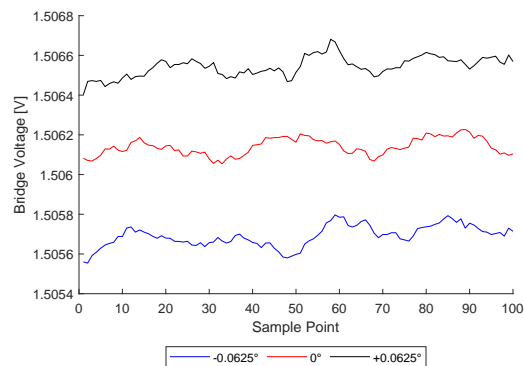
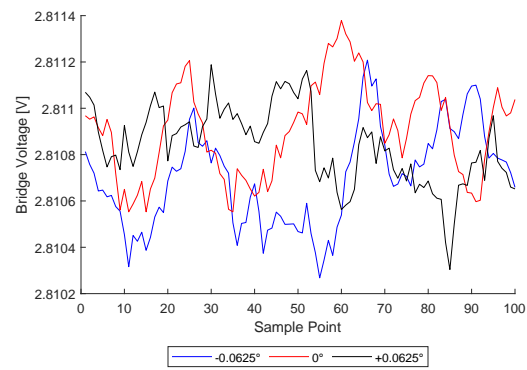Fig. A.2: Bridge voltages at calibrator from sensor 2 on SN71201083 at $-0.0625°$, $0°$, and $+0.0625°$ at 120 knots
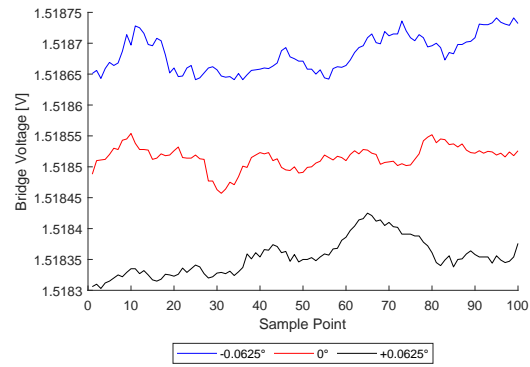
Fig. A.3: Bridge voltages at calibrator from sensor 1 on SN71201084 at $-0.0625°$, $0°$, and $+0.0625°$ at 120 knots
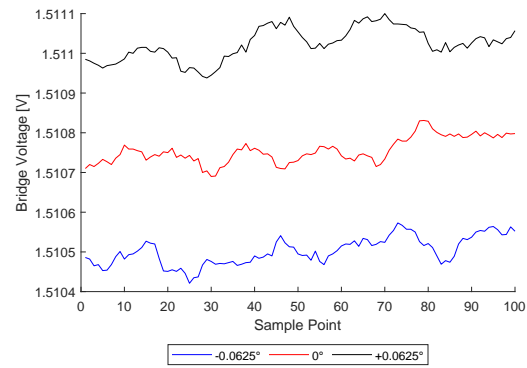
Fig. A.4: Bridge voltages at calibrator from sensor 2 on SN71201084 at $-0.0625°$, $0°$, and $+0.0625°$ at 120 knots
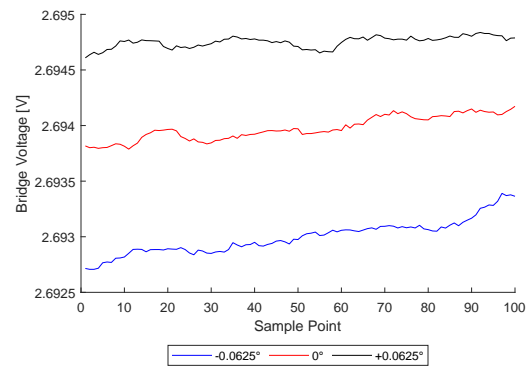
Fig. A.5: Bridge voltages at calibrator from sensor 1 on SN71201086 at $-0.0625°$, $0°$, and $+0.0625°$ at 120 knots
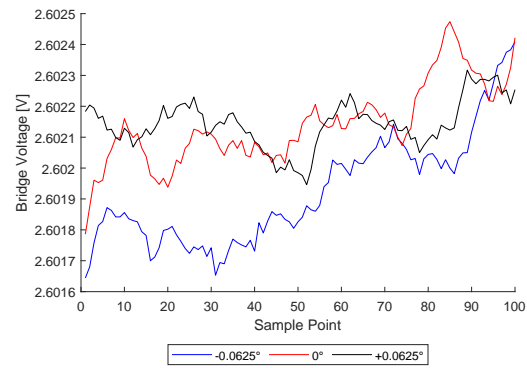
Fig. A.6: Bridge voltages at calibrator from sensor 2 on SN71201086 at $-0.0625°$, $0°$, and $+0.0625°$ at 120 knots
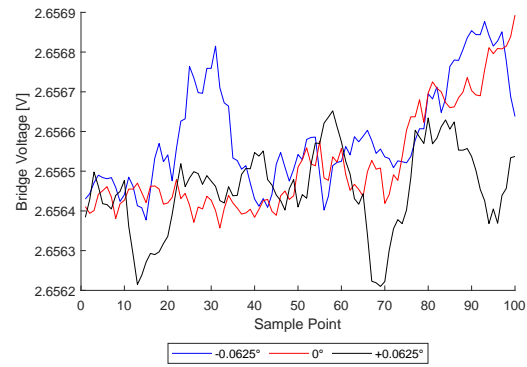
Fig. A.7: Bridge voltages at calibrator from sensor 1 on SN71327010 at $-0.0625°$, $0°$, and $+0.0625°$ at 120 knots
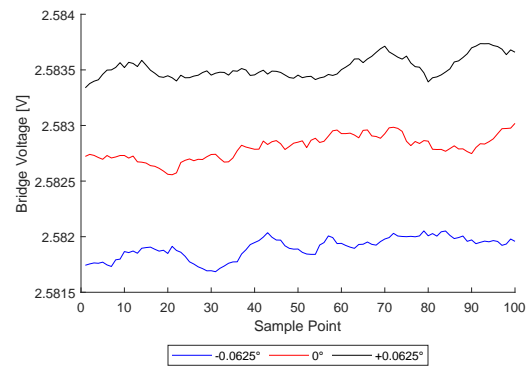
Fig. A.8: Bridge voltages at calibrator from sensor 2 on SN71327010 at $-0.0625°$, $0°$, and $+0.0625°$ at 120 knots
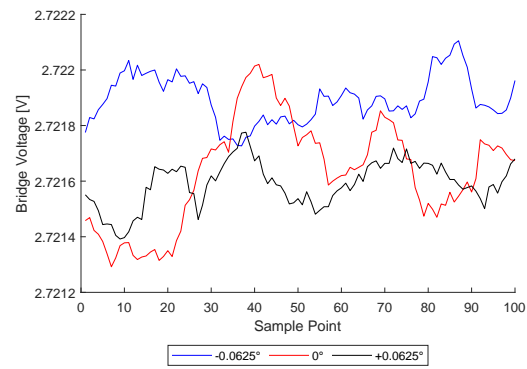
Fig. A.9: Bridge voltages at calibrator from sensor 1 on SN71327011 at $-0.0625°$, $0°$, and $+0.0625°$at 120 knots
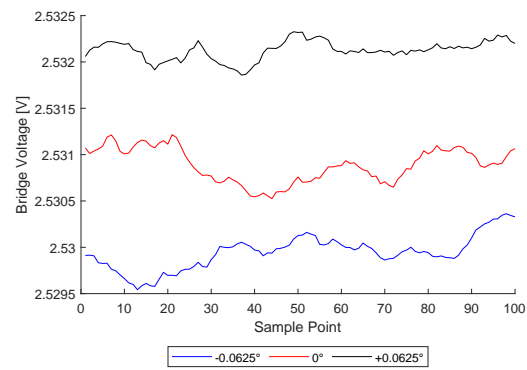
Fig. A.10: Bridge voltages at calibrator from sensor 2 on SN71327011 at $-0.0625°$, $0°$, and $+0.0625°$ at 120 knots
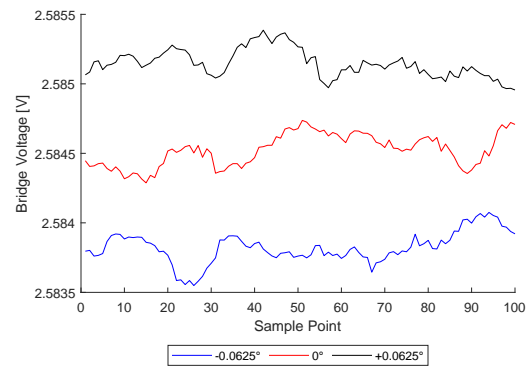
Fig. A.11: Bridge voltages at calibrator from sensor 1 on SN71430019 at $-0.0625°$, $0°$, and $+0.0625°$ at 120 knots
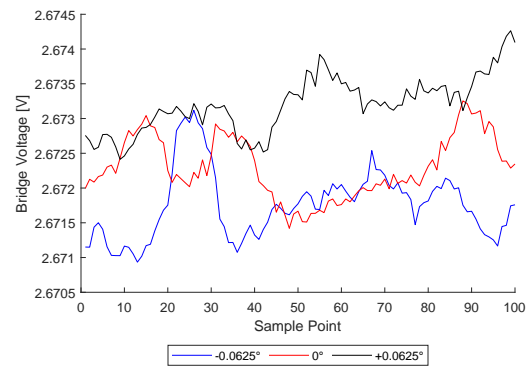
Fig. A.12: Bridge voltages at calibrator from sensor 2 on SN71430019 at $-0.0625°$, $0°$, and $+0.0625°$ at 120 knots

A.2 Rolling Average Voltages at 150 Knots
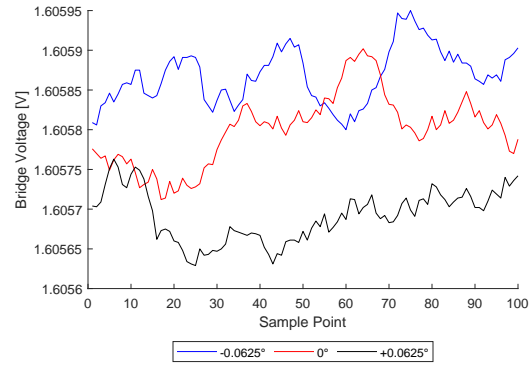
Fig. A.13: Bridge voltages at calibrator from sensor 1 on SN71201083 at $-0.0625°$, $0°$, and $+0.0625°$at 150 knots
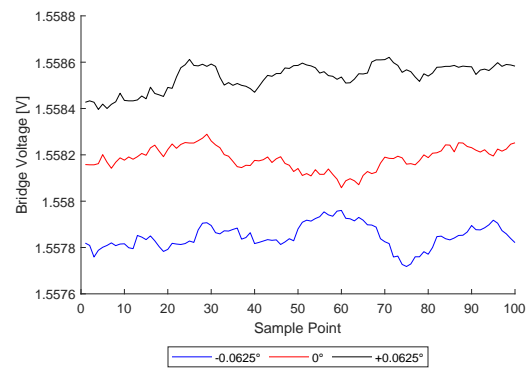
Fig. A.14: Bridge voltages at calibrator from sensor 2 on SN71201083 at $-0.0625°$, $0°$, and $+0.0625°$ at 150 knots
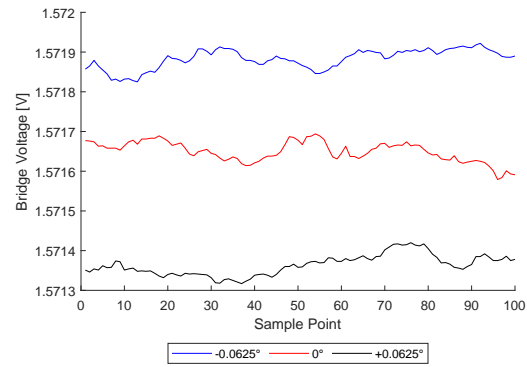
Fig. A.15: Bridge voltages at calibrator from sensor 1 on SN71201084 at −0.0625°, 0°, and +0.0625°at 150 knots
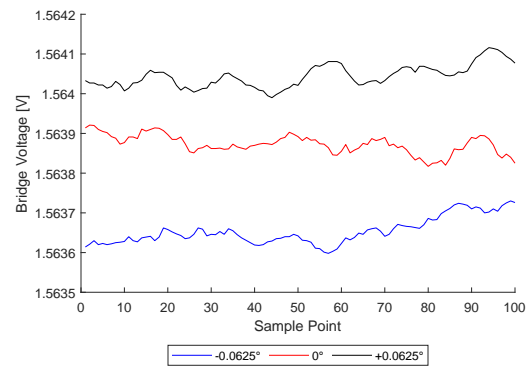
Fig. A.16: Bridge voltages at calibrator from sensor 2 on SN71201084 at −0.0625°, 0°, and +0.0625°at 150 knots
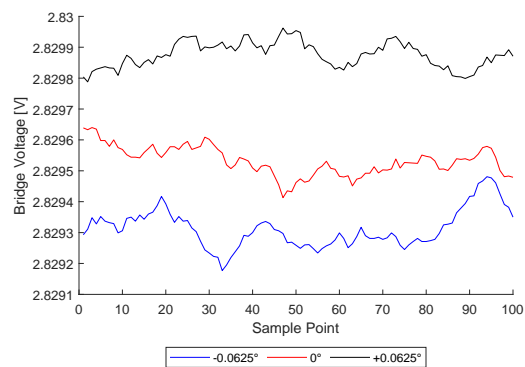
Fig. A.17: Bridge voltages at calibrator from sensor 1 on SN71201086 at $-0.0625°$, $0°$, and $+0.0625°$ at 150 knots
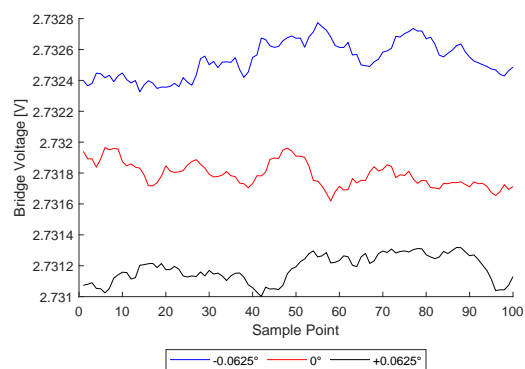
Fig. A.18: Bridge voltages at calibrator from sensor 2 on SN71201086 at $-0.0625°$, $0°$, and $+0.0625°$ at 150 knots
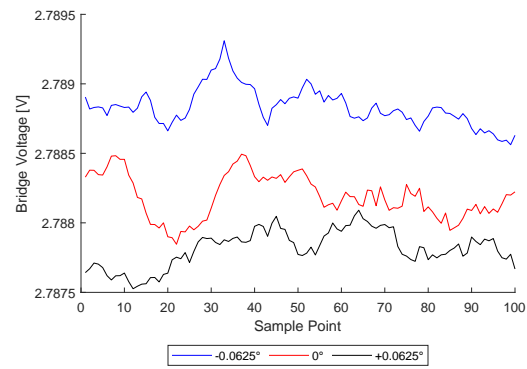
Fig. A.19: Bridge voltages at calibrator from sensor 1 on SN71327010 at $-0.0625°$, $0°$, and $+0.0625°$at 150 knots
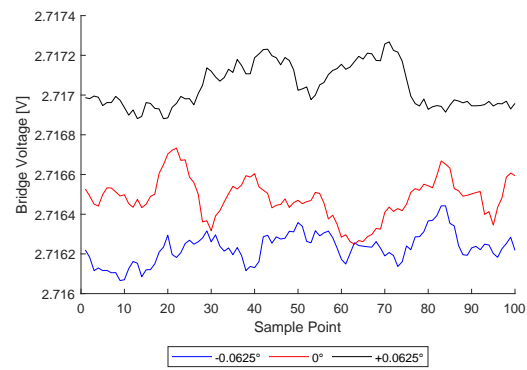
Fig. A.20: Bridge voltages at calibrator from sensor 2 on SN71327010 at $-0.0625°$, $0°$, and $+0.0625°$ at 150 knots

Fig. A.21: Bridge voltages at calibrator from sensor 1 on SN71327011 at $-0.0625°$, $0°$, and $+0.0625°$ at 150 knots

Fig. A.22: Bridge voltages at calibrator from sensor 2 on SN71327011 at $-0.0625°$, $0°$, and $+0.0625°$ at 150 knots

Fig. A.23: Bridge voltages at calibrator from sensor 1 on SN71430019 at $-0.0625°$, $0°$, and $+0.0625°$ at 150 knots

Fig. A.24: Bridge voltages at calibrator from sensor 2 on SN71430019 at $-0.0625°$, $0°$, and $+0.0625°$ at 150 knots
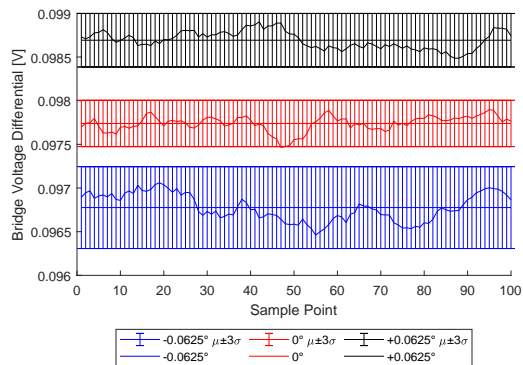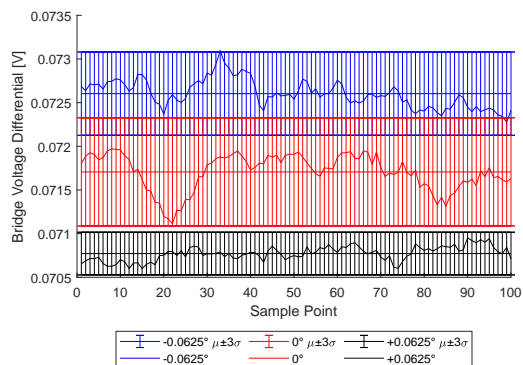
A.3   Differential Voltages at 120 knots
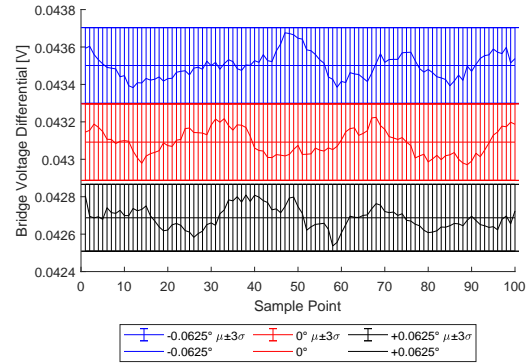
Fig. A.25: Differential bridge voltages at calibrator (sensor 2 bridge voltage minus sensor 1 bridge voltage) on SN71201083 at $-0.0625°$, $0°$, and $+0.0625°$ at 120 knots with $\pm3\sigma$ Standard Deviations
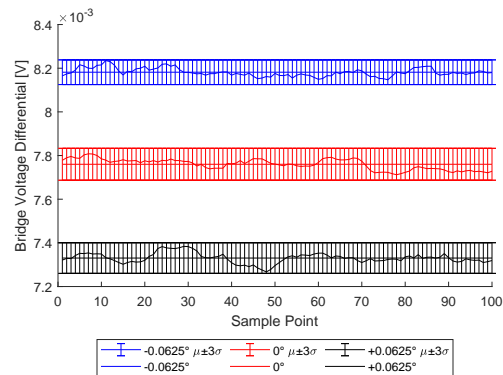
Fig. A.26: Differential bridge voltages at calibrator (sensor 2 bridge voltage minus sensor 1 bridge voltage) on SN71201084 at $-0.0625°$, $0°$, and $+0.0625°$ at 120 knots with $\pm3\sigma$ Standard Deviations
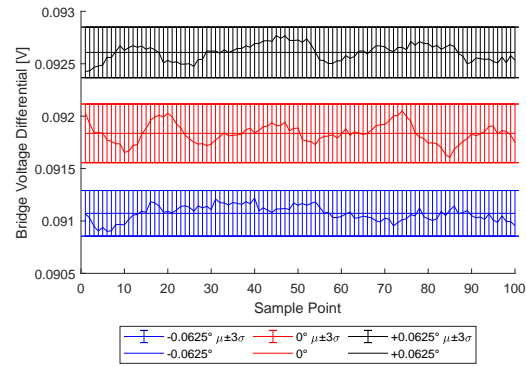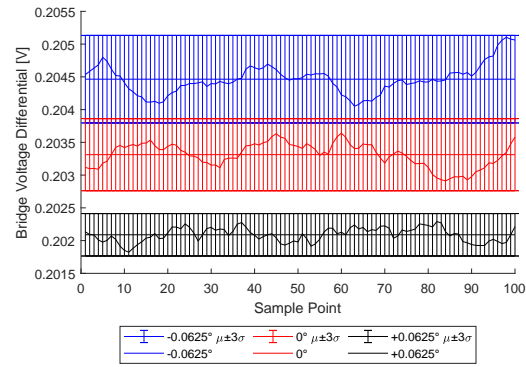
Fig. A.27: Differential bridge voltages at calibrator (sensor 2 bridge voltage minus sensor 1 bridge voltage) on SN71201086 at $-0.0625°$, $0°$, and $+0.0625°$at 120 knots with $\pm 3\sigma$ Standard Deviations
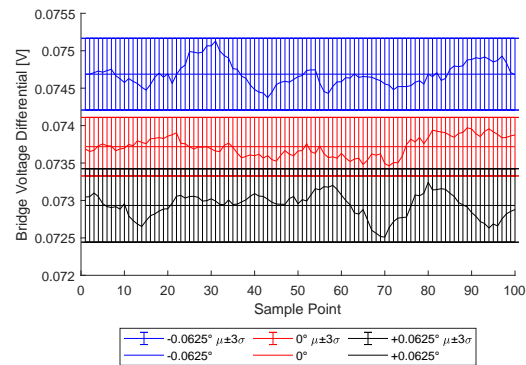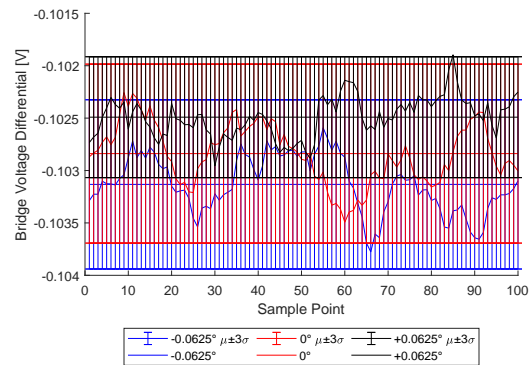

Fig. A.28: Differential bridge voltages at calibrator (sensor 2 bridge voltage minus sensor 1 bridge voltage) on SN71327010 at $-0.0625°$, $0°$, and $+0.0625°$at 120 knots with $\pm 3\sigma$ Standard Deviations
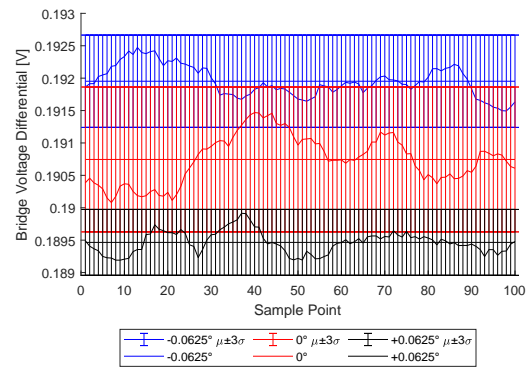
Fig. A.29: Differential bridge voltages at calibrator (sensor 2 bridge voltage minus sensor 1 bridge voltage) on SN71327011 at $-0.0625°$, $0°$, and $+0.0625°$ at 120 knots with $\pm 3\sigma$ Standard Deviations
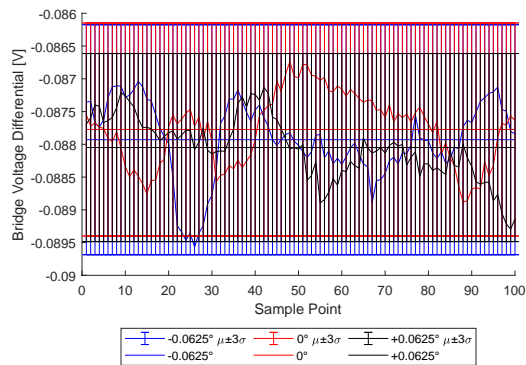
Fig. A.30: Differential bridge voltages at calibrator (sensor 2 bridge voltage minus sensor 1 bridge voltage) on SN71430019 at $-0.0625°$, $0°$, and $+0.0625°$ at 120 knots with $\pm 3\sigma$ Standard Deviations

A.4 Differential Voltages at 150 knots
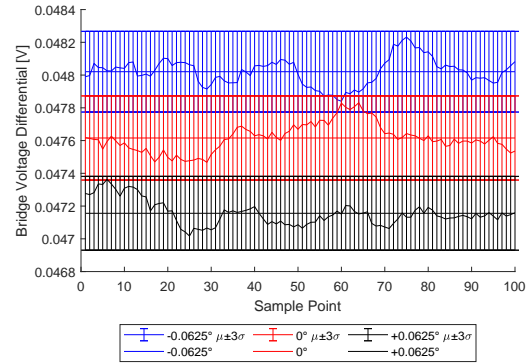
Fig. A.31: Differential bridge voltages at calibrator (sensor 2 bridge voltage minus sensor 1 bridge voltage) on SN71201083 at $-0.0625°$, $0°$, and $+0.0625°$at 150 knots with $\pm 3\sigma$ Standard Deviations
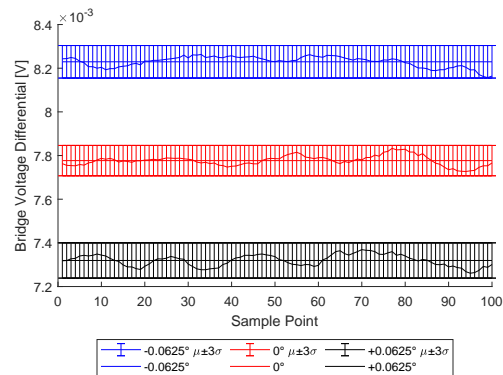
Fig. A.32: Differential bridge voltages at calibrator (sensor 2 bridge voltage minus sensor 1 bridge voltage) on SN71201084 at $-0.0625°$, $0°$, and $+0.0625°$at 150 knots with $\pm 3\sigma$ Standard Deviations

Fig. A.33: Differential bridge voltages at calibrator (sensor 2 bridge voltage minus sensor 1 bridge voltage) on SN71201086 at $-0.0625°$, $0°$, and $+0.0625°$at 150 knots with $\pm3\sigma$ Standard Deviations

Fig. A.34: Differential bridge voltages at calibrator (sensor 2 bridge voltage minus sensor 1 bridge voltage) on SN71327010 at $-0.0625°$, $0°$, and $+0.0625°$at 150 knots with $\pm3\sigma$ Standard Deviations

Fig. A.35: Differential bridge voltages at calibrator (sensor 2 bridge voltage minus sensor 1 bridge voltage) on SN71327011 at $-0.0625°$, $0°$, and $+0.0625°$ at 150 knots with $\pm 3\sigma$ Standard Deviations

Fig. A.36: Differential bridge voltages at calibrator (sensor 2 bridge voltage minus sensor 1 bridge voltage) on SN71430019 at $-0.0625°$, $0°$, and $+0.0625°$ at 150 knots with $\pm 3\sigma$ Standard Deviations

A.5 Rolling Average Voltages at 50 knots
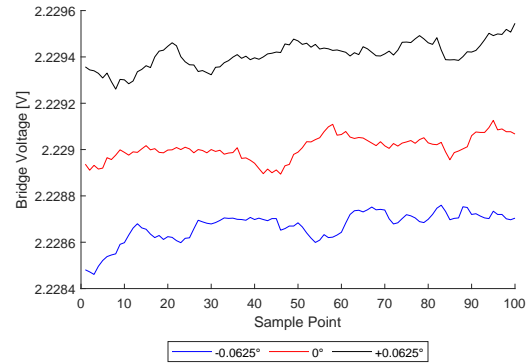
Fig. A.37: Bridge voltages at calibrator from sensor 1 on SN71201086 at $-0.0625°$, $0°$, and $+0.0625°$ at 50 knots
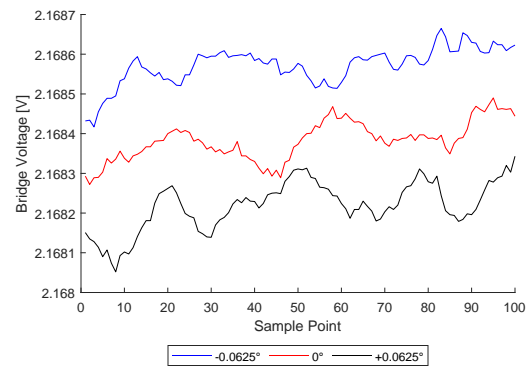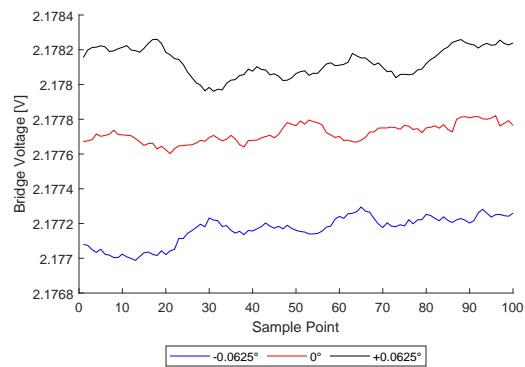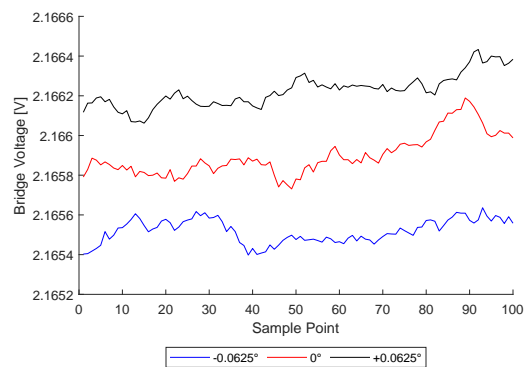

Fig. A.38: Bridge voltages at calibrator from sensor 2 on SN71201086 at $-0.0625°$, $0°$, and $+0.0625°$ at 50 knots
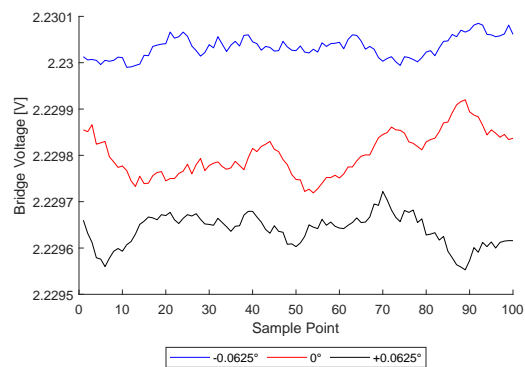
Fig. A.39: Bridge voltages at calibrator from sensor 1 on SN71327010 at −0.0625°, 0°, and +0.0625°at 50 knots
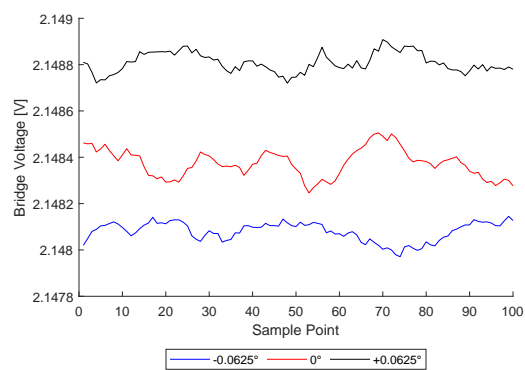
Fig. A.40: Bridge voltages at calibrator from sensor 2 on SN71327010 at −0.0625°, 0°, and +0.0625°at 50 knots
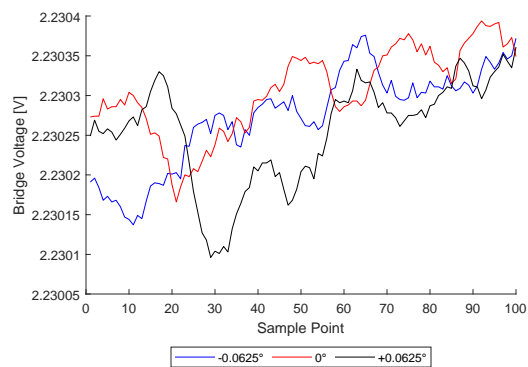
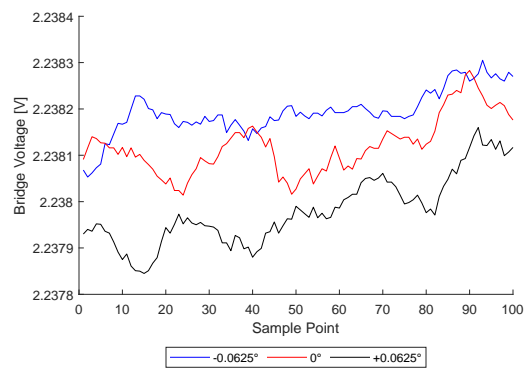Fig. A.41: Bridge voltages at calibrator from sensor 1 on SN71327011 at −0.0625°, 0°, and +0.0625° at 50 knots

Fig. A.42: Bridge voltages at calibrator from sensor 2 on SN71327011 at −0.0625°, 0°, and +0.0625° at 50 knots

Fig. A.43: Bridge voltages at calibrator from sensor 1 on SN71430019 at $-0.0625°$, $0°$, and $+0.0625°$ at 50 knots

Fig. A.44: Bridge voltages at calibrator from sensor 2 on SN71430019 at $-0.0625°$, $0°$, and $+0.0625°$ at 50 knots

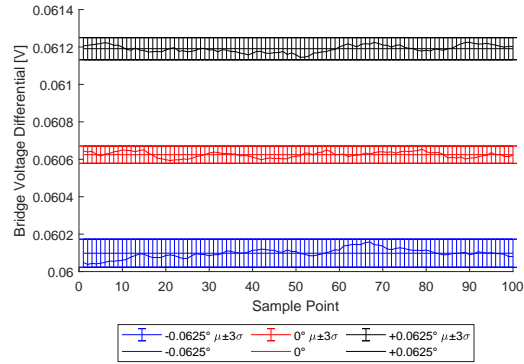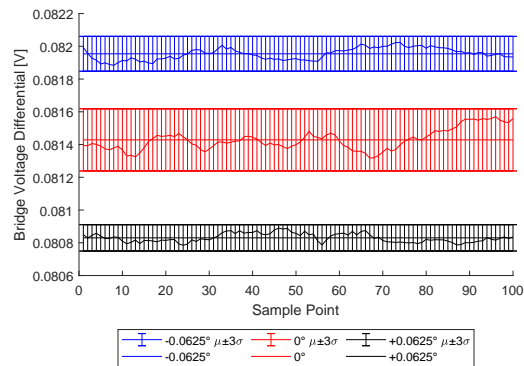## A.6 Differential Voltages at 50 knots

Fig. A.45: Differential bridge voltages at calibrator (sensor 2 bridge voltage minus sensor 1 bridge voltage) on SN71201086 at $-0.0625°$, $0°$, and $+0.0625°$ at 50 knots with $\pm3\sigma$ Standard Deviations
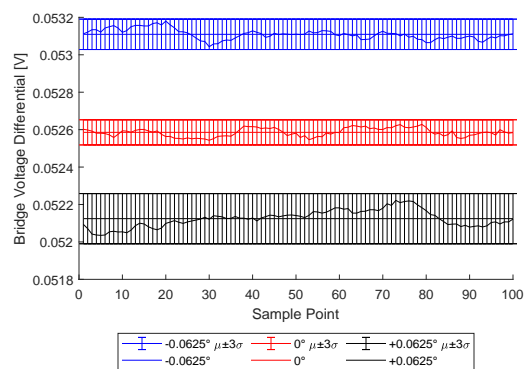

Fig. A.46: Differential bridge voltages at calibrator (sensor 2 bridge voltage minus sensor 1 bridge voltage) on SN71327010 at $-0.0625°$, $0°$, and $+0.0625°$ at 50 knots with $\pm3\sigma$ Standard Deviations

Fig. A.47: Differential bridge voltages at calibrator (sensor 2 bridge voltage minus sensor 1 bridge voltage) on SN71327011 at $-0.0625°$, $0°$, and $+0.0625°$at 50 knots with $\pm3\sigma$ Standard Deviations
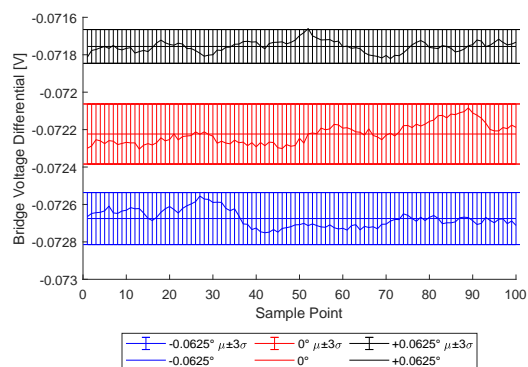

Fig. A.48: Differential bridge voltages at calibrator (sensor 2 bridge voltage minus sensor 1 bridge voltage) on SN71430019 at $-0.0625°$, $0°$, and $+0.0625°$at 50 knots with $\pm3\sigma$ Standard Deviations